7th International Workshop on Multiple Partonic Interactions at the LHC
23 - 27 November 2015 Miramare, Trieste, Italy

Multi-Parton Interactions in p-Pb collisions at $\sqrt{s_{NN}}$ = 5.02 TeV with ALICE

C. Oppedisano
on behalf of the ALICE Collaboration

MPI: from pp to p-A

pp ➧ high multiplicity events arise from low impact parameter collisions and statistical upward fluctuations of the number of MPI per event

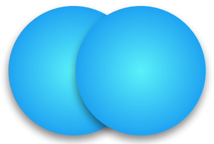

MPI expected to be enhanced in collisions with nuclei (larger transverse parton density, larger number of hadron-hadron collisions) at high energies (lower parton momentum fraction)

A-A ➧ number of MPI largely determined by centrality (large N_{coll})

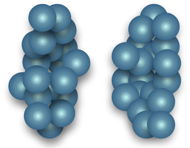

p-A ➧ parton-parton scatterings determined by p-A centrality
BUT since N_{coll} values are small also pN geometry becomes important!

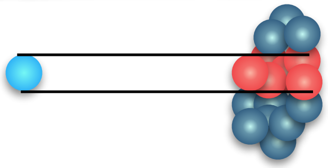

From pp to p-A
➧ larger number of MPI per event due to larger $\langle N_{coll} \rangle$, with an overlap reaction region of similar size as in pp
➧ use what we learnt from pp high multiplicity as a reference for p-A

MPI: from pp to p-A

ALICE Coll., arXiv:nucl-ex 1509.08734

Events with a high p_T particle correspond to more central pp collisions (high multiplicity)

- selecting high p_T particles more central collisions are selected
- in p-A, a selection based on multiplicity can bias the estimate of the number of hard scatterings per binary collision

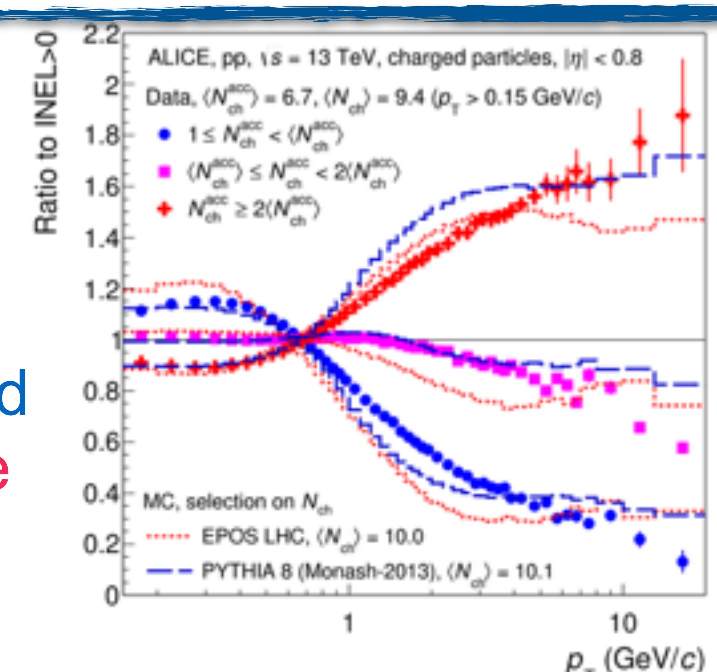

MPI: from pp to p-A

ALICE Coll., arXiv:nucl-ex 1509.08734

Events with a high p_T particle correspond to more central pp collisions (high multiplicity)

- selecting high p_T particles more central collisions are selected
- in p-A, a selection based on multiplicity can bias the estimate of the number of hard scatterings per binary collision

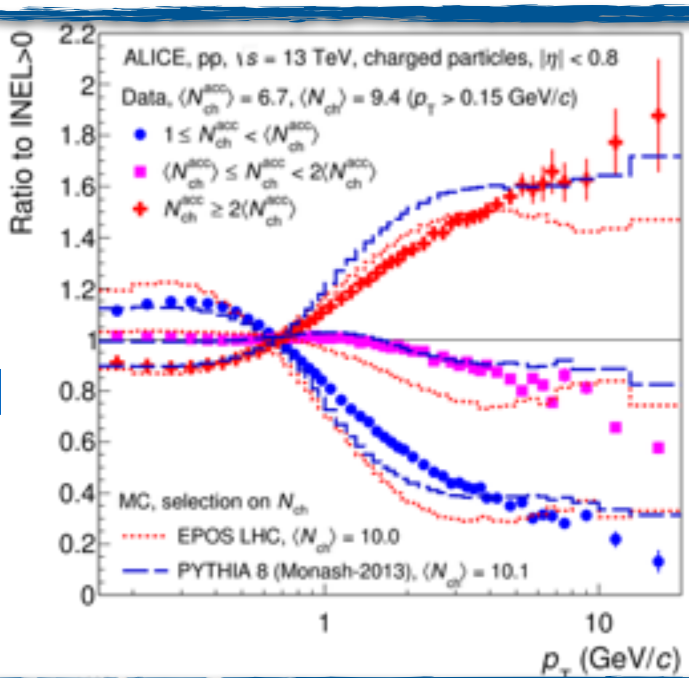

In a factorization approach:

- $$< n_{hard} >^{pN} = < \mathrm{N}_{\mathrm{coll}}^{\mathrm{Glauber}} >^{\mathrm{MB}} \cdot < n_{hard} >^{pp}$$
- yields from hard processes per binary collision scale like:

$$\frac{\mathrm{Y}_{\mathrm{hard}}}{<\mathrm{N}_{\mathrm{coll}}^{\mathrm{Glauber}}>} \sim \frac{<n_{hard}>^{pN}}{<n_{hard}>^{pp}}$$

=1 for centrality integrated p-A collisions
can deviate from unity in centrality selected classes

MPI: from pp to p-A

ALICE Coll., arXiv:nucl-ex 1509.08734

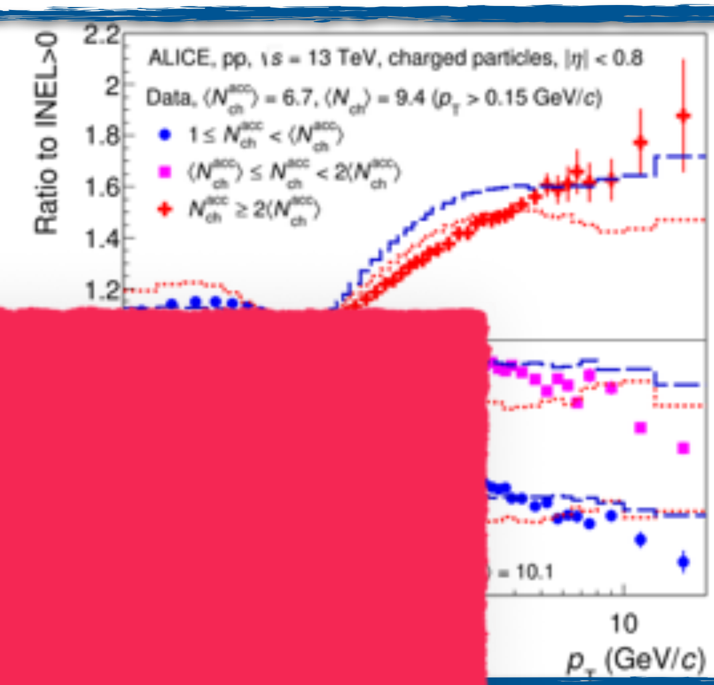

Events with a high p_T particle correspond to more central pp collision

- selecti
- in p-A
of the n

- OUTLINE OF THE PRESENTATION
- Centrality selection and biases
- MPI through two-particle jet-like correlations

In a fact

- $< n_h$
- yields

$$\frac{Y_{hard}}{<N_{coll}^{Glauber}>} \sim \frac{<n_{hard}>^{pN}}{<n_{hard}>^{pp}}$$

=1 for centrality integrated p-A collisions
can deviate from unity in centrality selected classes

Centrality determination

Centrality ➧ classification of collision geometry based on a measured observable (with a monotonic correlation with collision geometry ⇔ b, N_{coll}, N_{part})

Centrality estimator M related to geometry through Glauber convoluted with a model to describe the observable (NBD for particle production, Γ function for E_T)

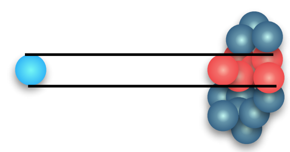

Glauber MC: $P(N_{coll})$

⊗

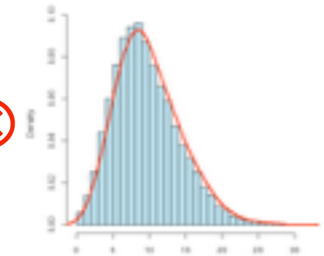

Model: $P(M|N_{coll})$

- ➧ conditional probability $P(M \mid N_{coll})$
- ➧ classify events as percentiles of cross-section
- ➧ $\langle N_{part} \rangle$ and $\langle N_{coll} \rangle$ in each centrality bin

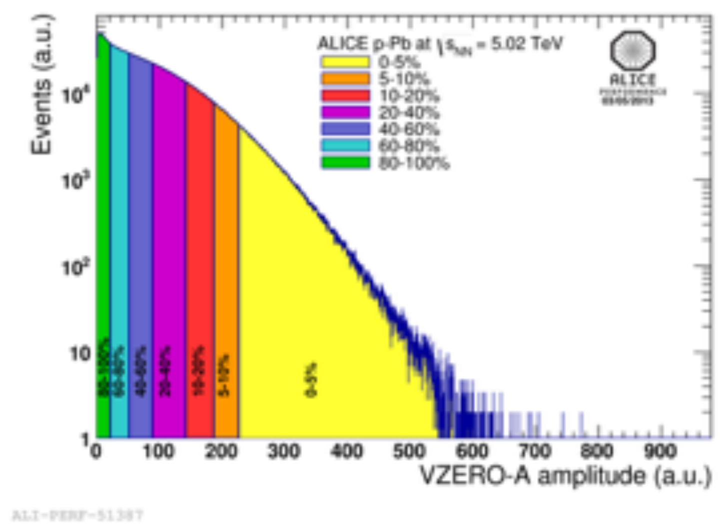

Centrality determination

Centrality ➧ classification of collision geometry based on a measured observable (with a monotonic correlation with collision geometry ⇔ b, N_{coll}, N_{part})

Centrality estimator M related to geometry through Glauber convoluted with a model to describe the observable (NBD for particle production, Γ function for E_T)

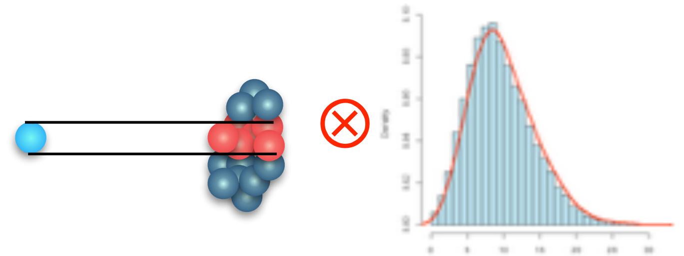

Glauber MC: $P(N_{coll})$ ⊗ Model: $P(M|N_{coll})$

➧ conditional probability $P(M \mid N_{coll})$

➧ classify events as percentiles of cross-section

➧ $\langle N_{part}\rangle$ and $\langle N_{coll}\rangle$ in each centrality bin

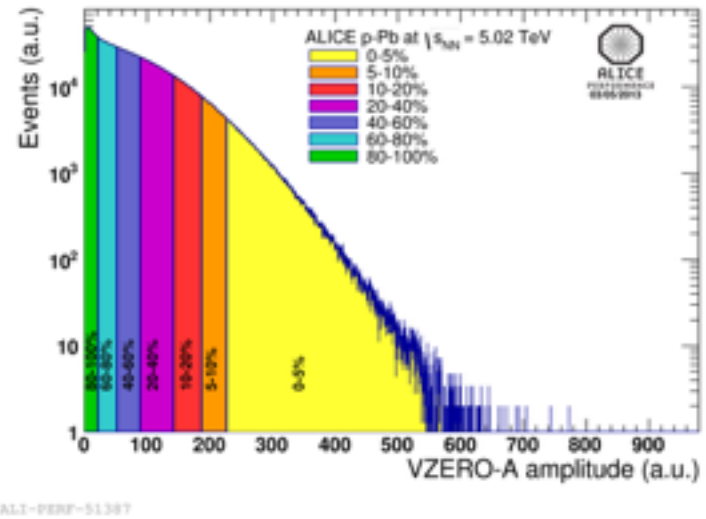

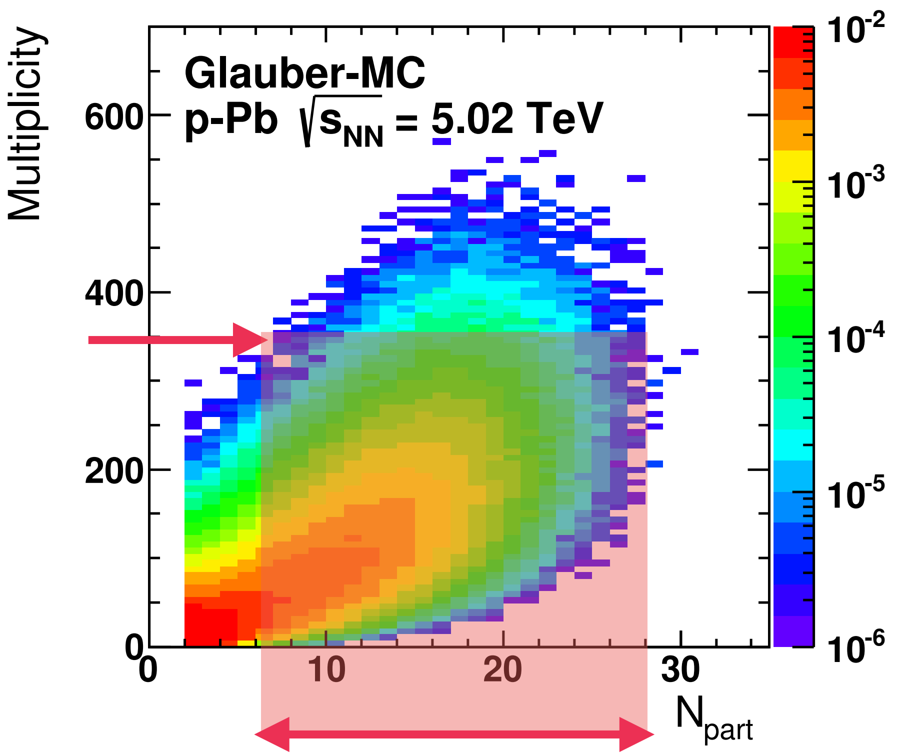

☐ check if the centrality selection could induce a bias in the geometry parameters ➧ selection in a system with large relative fluctuations can induce a bias

Centrality determination

Centrality ➧ classification of collision geometry based on a measured observable (with a monotonic correlation with collision geometry ⇔ b, N_{coll}, N_{part})

Centrality estimator M related to geometry through Glauber convoluted with a model to describe the observable (NBD for particle production, Γ function for E_T)

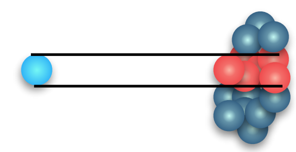
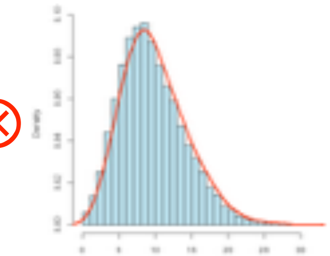

Glauber MC: $P(N_{coll})$ ⊗ Model: $P(M|N_{coll})$

- ➧ conditional probability $P(M | N_{coll})$
- ➧ classify events as percentiles of cross-section
- ➧ $\langle N_{part}\rangle$ and $\langle N_{coll}\rangle$ in each centrality bin

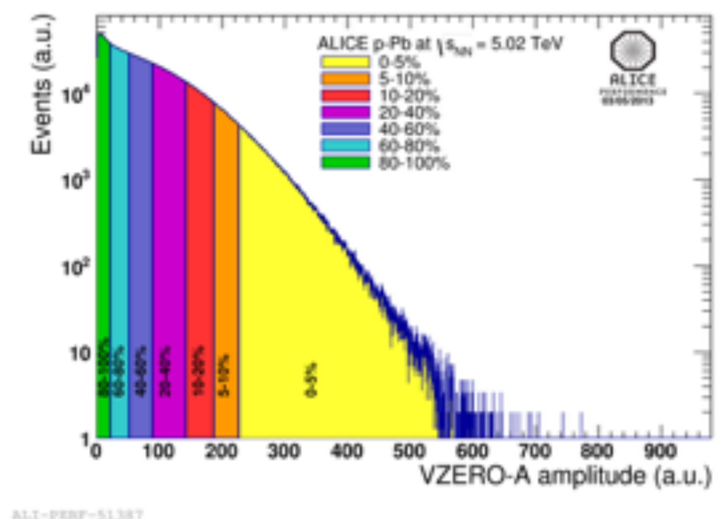

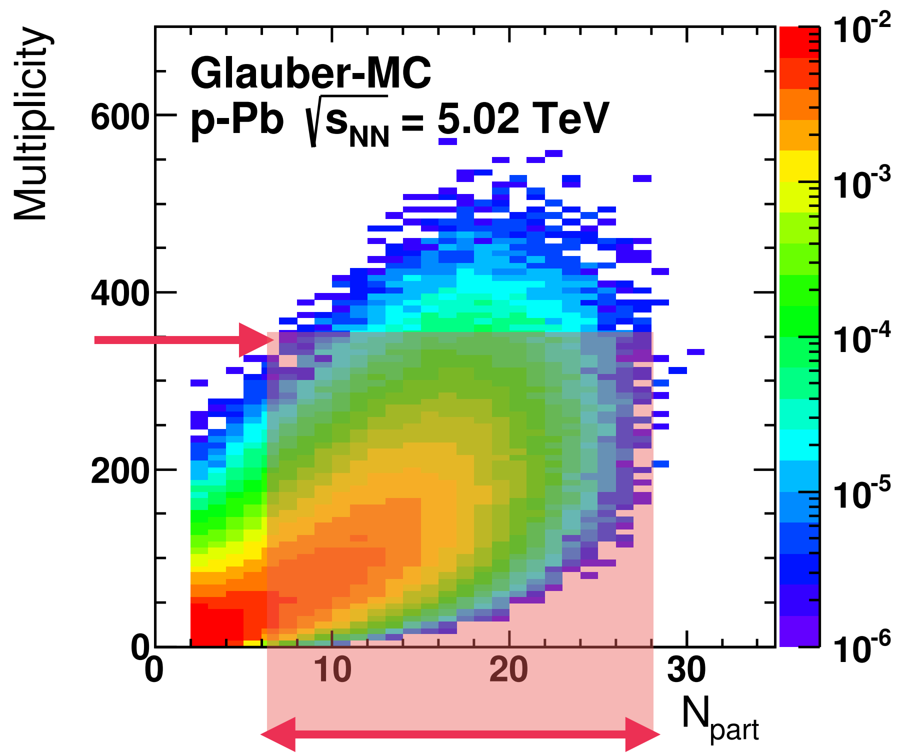

- ❏ check if the centrality selection could induce a bias in the geometry parameters ➧ selection in a system with large relative fluctuations can induce a bias
- ❏ verify the connection between estimator and geometry comparing Glauber MC and data for a known process or correlating observables from kinematic regions that are causally disconnected after collision

Centrality estimators

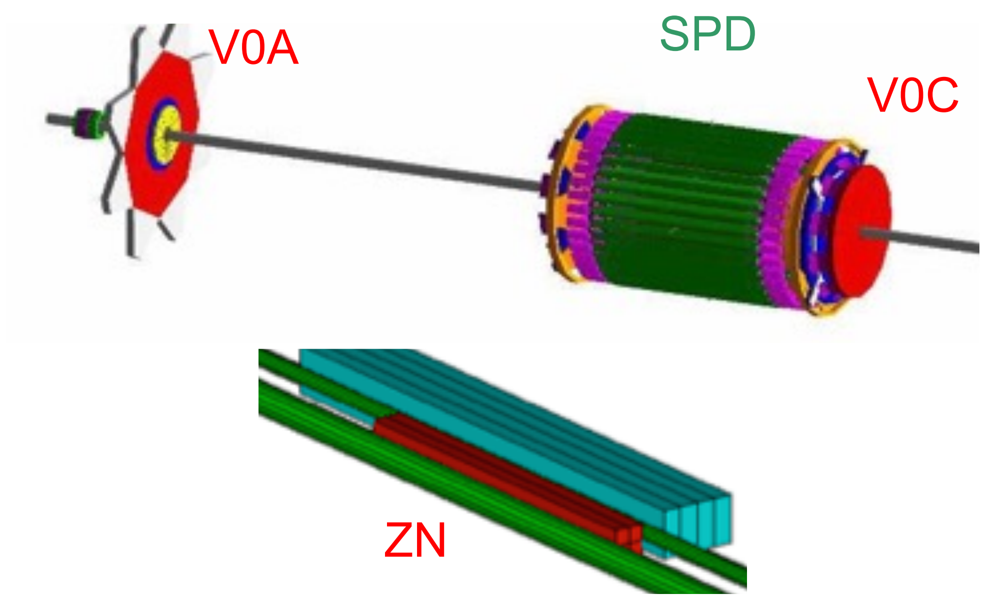

✱ DETECTORS

- @ midrapidity ➧ 2 inner ITS pixel layers |η|< 2, |η|<1.4
- @ forward rapidities ➧ V0 scintillator hodoscopes
  V0A 2.0<η<5.1 V0C -3.7<η<-1.7
- @ beam rapidity ➧ neutron ZDC (ZN) |η|>8.7

Centrality estimators

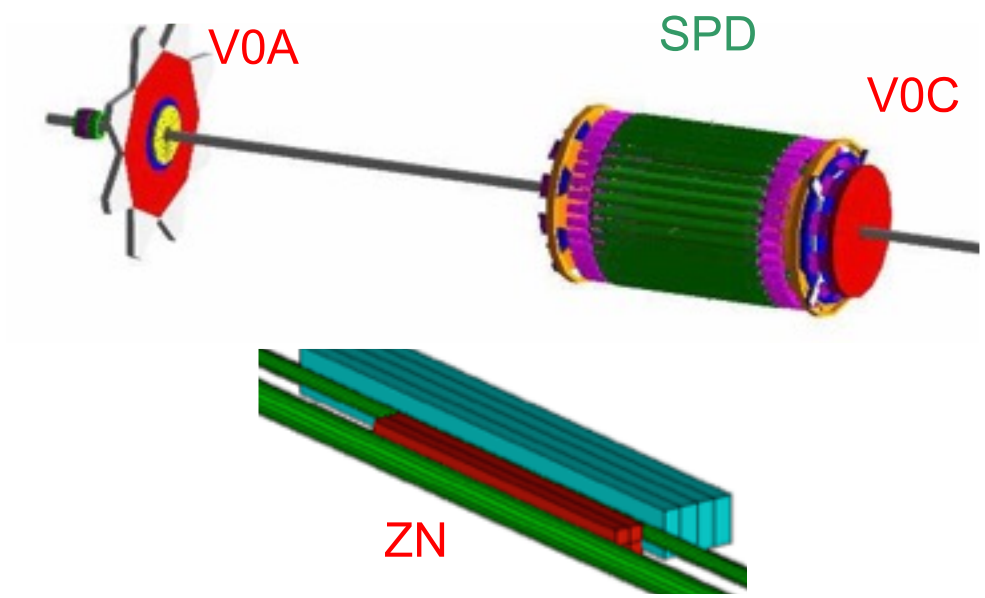

✱ DETECTORS

- @ midrapidity ➧ 2 inner ITS pixel layers |η|< 2, |η|<1.4
- @ forward rapidities ➧ V0 scintillator hodoscopes
  V0A 2.0<η<5.1 V0C -3.7<η<-1.7
- @ beam rapidity ➧ neutron ZDC (ZN) |η|>8.7

✱ ESTIMATORS

CL1 ➧ number of clusters in 2nd pixel layer
V0C ➧ raw multiplicity in p-side V0
V0A ➧ raw multiplicity in Pb-side V0
ZNA ➧ ZN energy on Pb-side

ALICE Coll., Phys. Rev. C 91 (2015) 064905

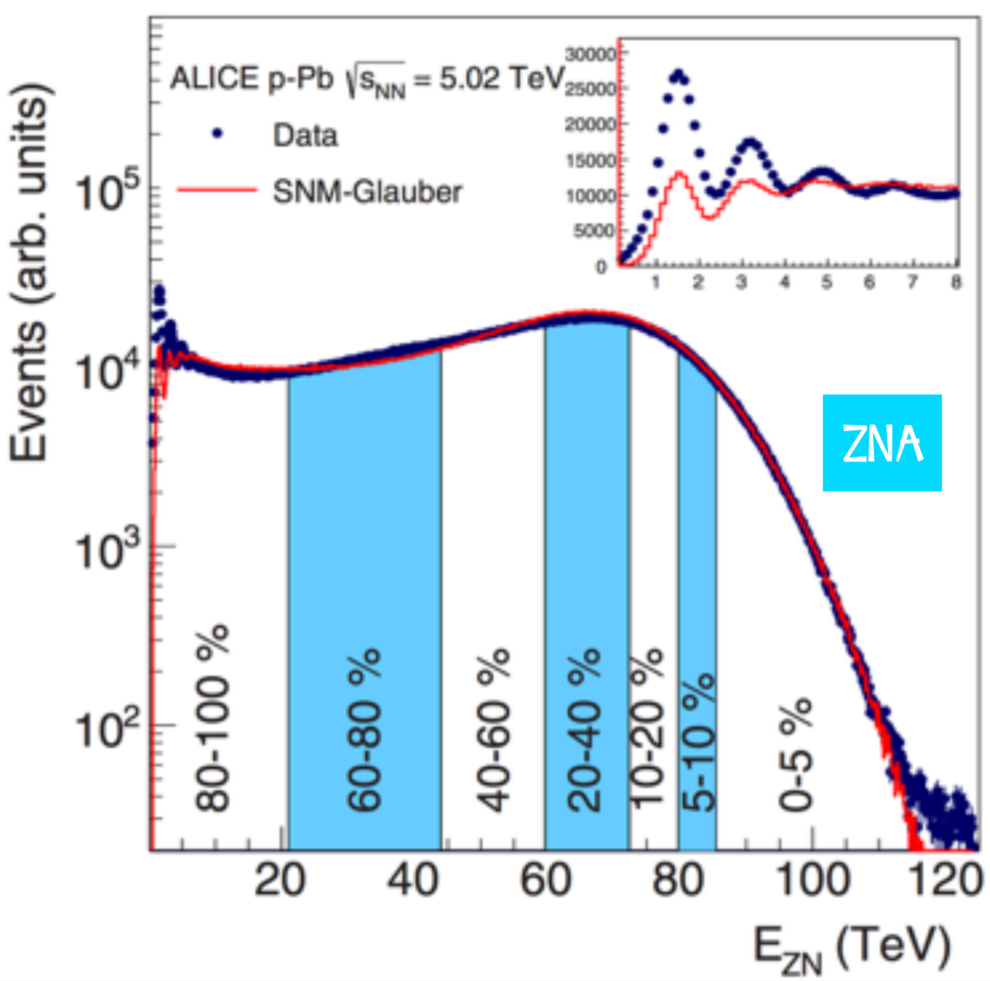

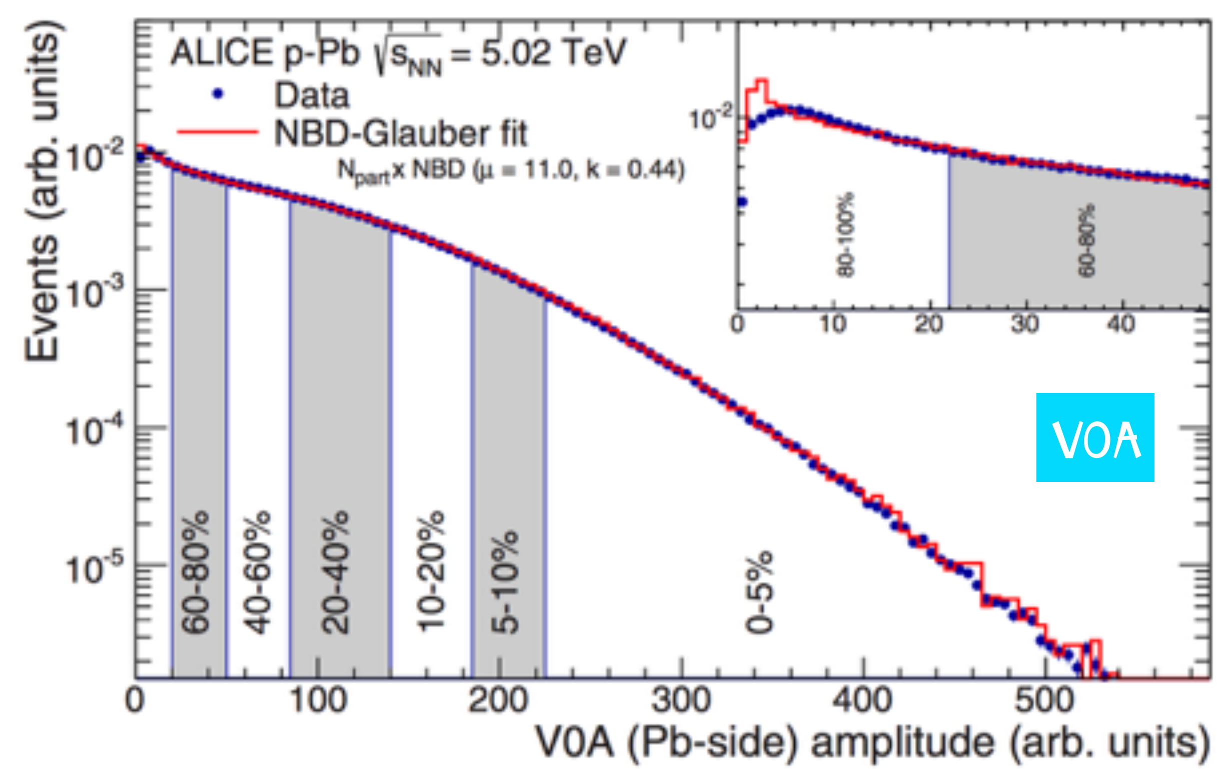

Bias sources (I)

- Multiplicity bias

Large multiplicity fluctuations ➧ centrality selection based on multiplicity may select a biased sample of NN collisions

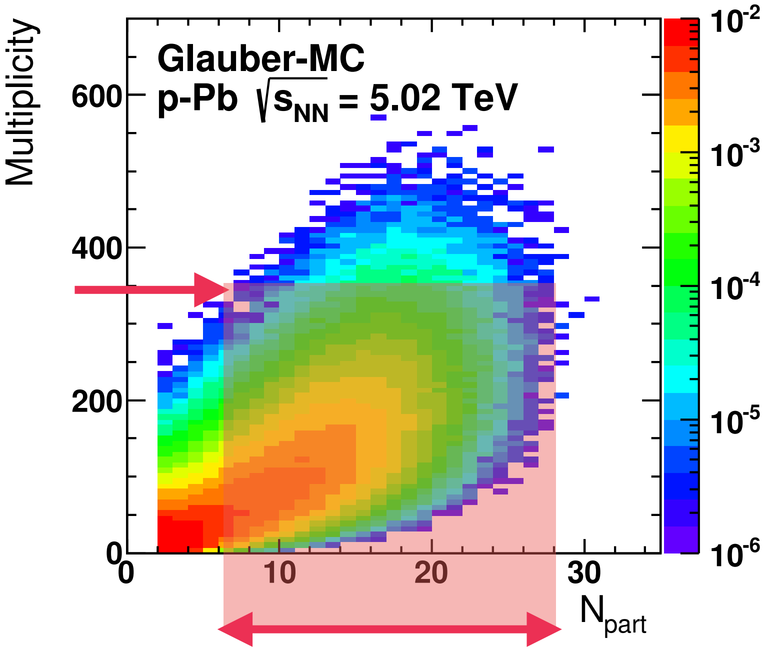

Bias sources (I)

- Multiplicity bias

Large multiplicity fluctuations ➧ centrality selection based on multiplicity may select a biased sample of NN collisions

- Multiplicity bias through Glauber fit

Mean multiplicity x participant / μ from NBD
➧ central (peripheral) collisions have larger (smaller) multiplicity per N_{part} than average

ALICE Coll., Phys. Rev. C 91 (2015) 064905

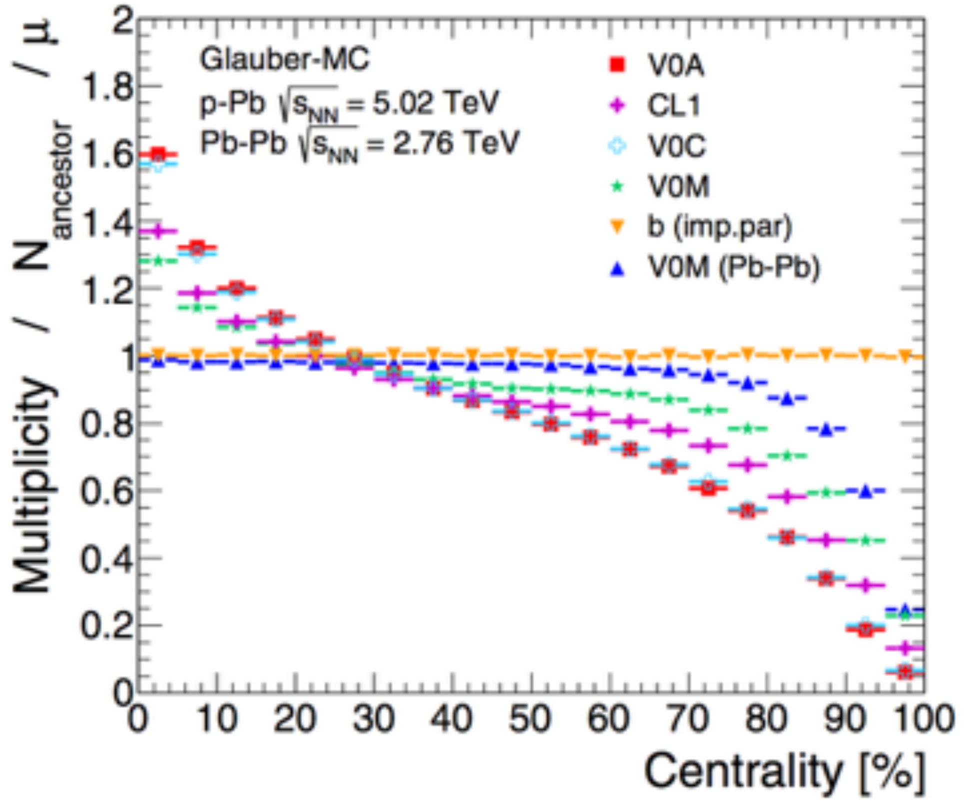

Bias sources (I)

Multiplicity bias

Large multiplicity fluctuations ➧ centrality selection based on multiplicity may select a biased sample of NN collisions

ALICE Coll., Phys. Rev. C 91 (2015) 064905

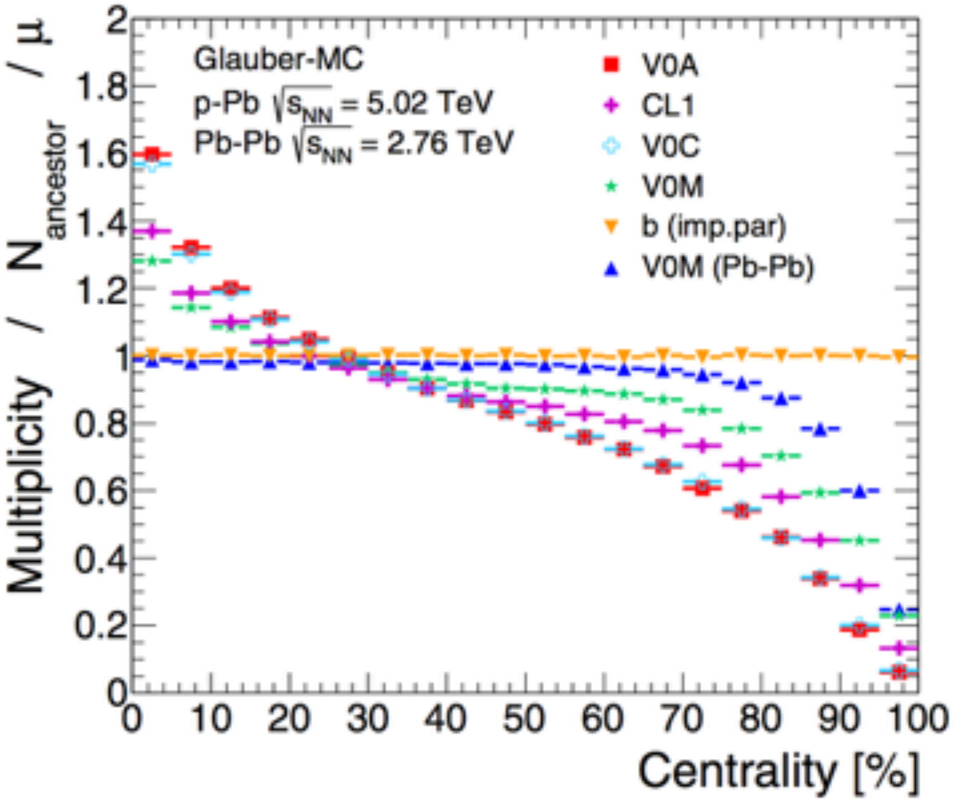

- Multiplicity bias through Glauber fit
  Mean multiplicity x participant / μ from NBD
  ➧ central (peripheral) collisions have larger (smaller) multiplicity per N_{part} than average

- Multiplicity bias through HIJING
  Multiplicity fluctuations due to fluctuations in MPIs
  $\langle n_{hard} \rangle = \sigma_{hard} * T_{NN}(b_{NN})$
  ➧ the bias on multiplicity corresponds to a bias on n_{hard}

Bias sources (I)

Multiplicity bias

Large multiplicity fluctuations ➧ centrality selection based on multiplicity may select a biased sample of NN collisions

ALICE Coll., Phys. Rev. C 91 (2015) 064905

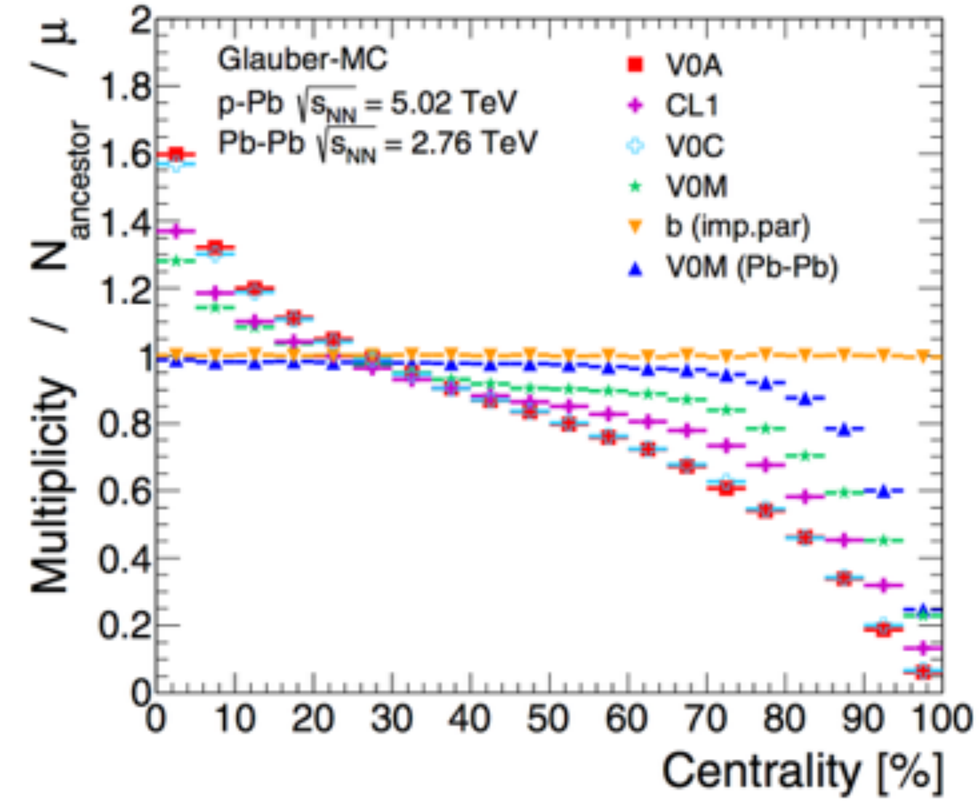

- Multiplicity bias through Glauber fit
  Mean multiplicity x participant / μ from NBD
  ➧ central (peripheral) collisions have larger (smaller) multiplicity per N_{part} than average

- Multiplicity bias through HIJING
  Multiplicity fluctuations due to fluctuations in MPIs
  $\langle n_{hard} \rangle = \sigma_{hard} * T_{NN}(b_{NN})$
  ➧ the bias on multiplicity corresponds to a bias on n_{hard}

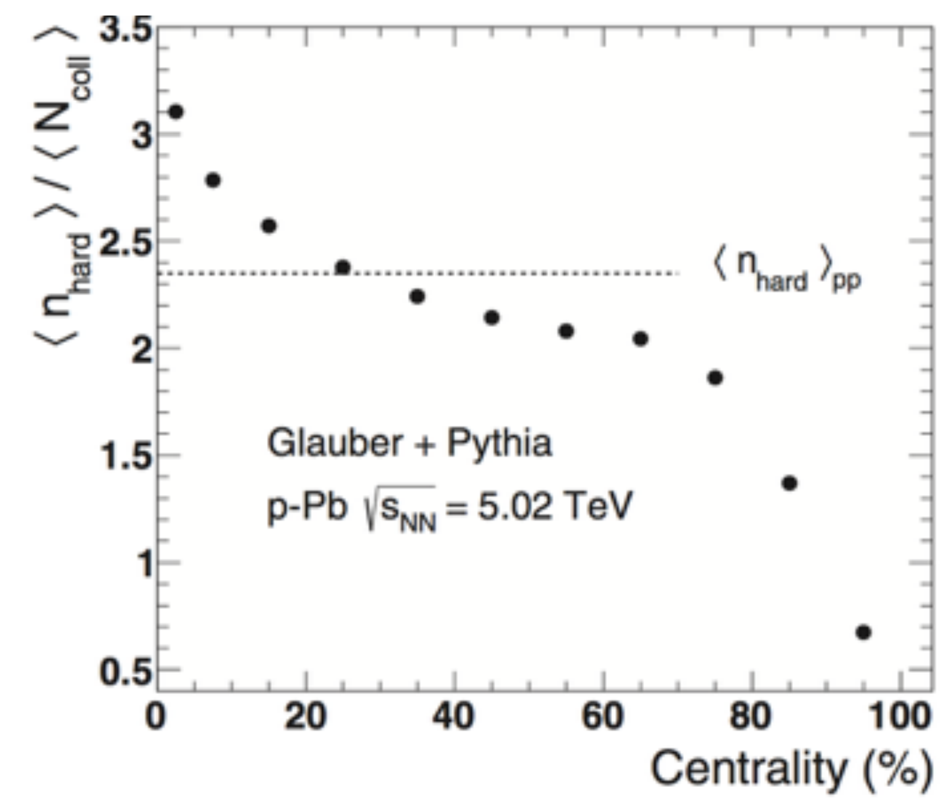

G-PYTHIA
Incoherent superposition of N-N PYTHIA collisions coupled to Glauber MC
➧ $\langle n_{hard} \rangle$ per pN collision deviates from N_{coll} scaling

Bias sources (II)

- Jet-veto bias

Kinematic bias

- high-p_T particles contribute to overall multiplicity and shift event to higher centralities
- larger bias when centrality estimator overlaps with the region where tracks are measured (CL1)

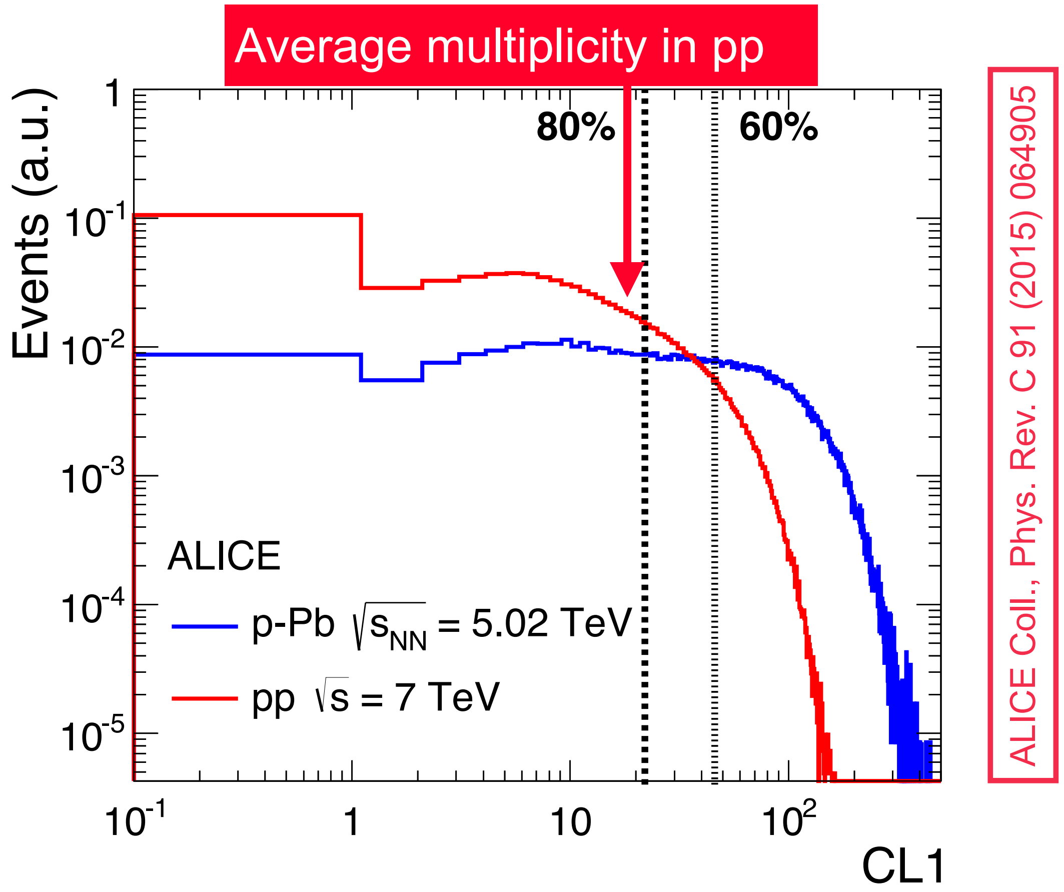

- Geometric bias

See also J. Jia, arXiv:0907.4175

Purely geometric bias

- in peripheral collisions $\langle b_{NN} \rangle$ is larger
- smaller than average number of MPIs
- independent of centrality estimator

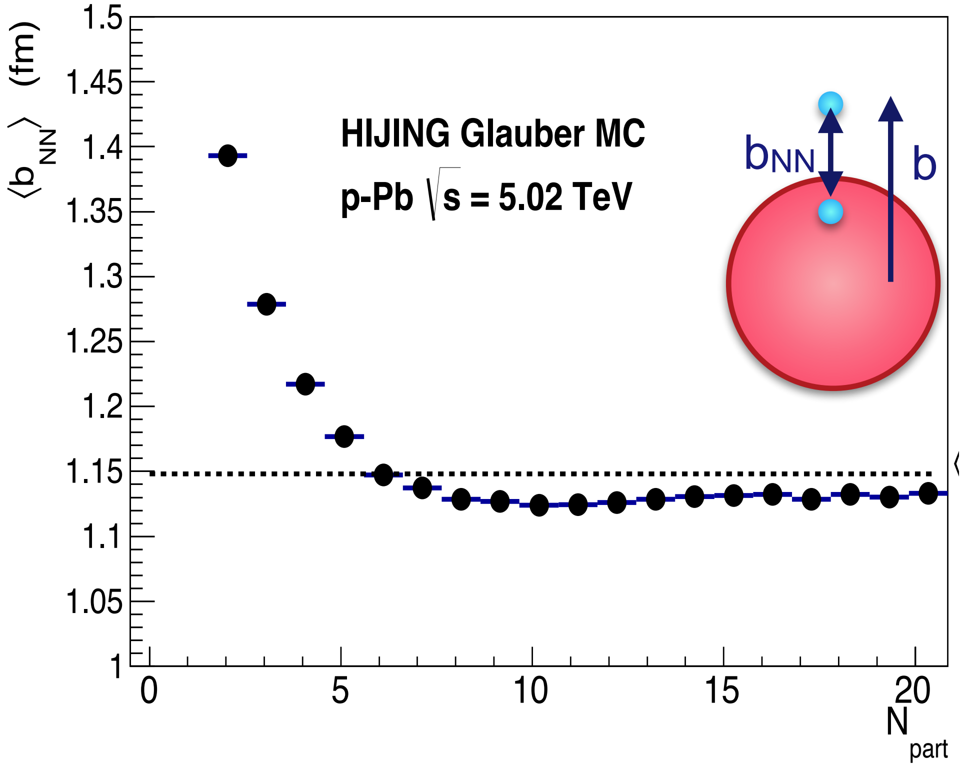

Bias at high p_T

Deviations from binary scaling at high p_T expected

➧ central (enhanced yield ➧ $R_{pA}>1$) and peripheral (lower yield ➧ $R_{pA}<1$) classes

➧ G-PYTHIA incoherent superposition of NN collisions

➧ $Q_{pPb} = R_{pPb}$ including possible biases

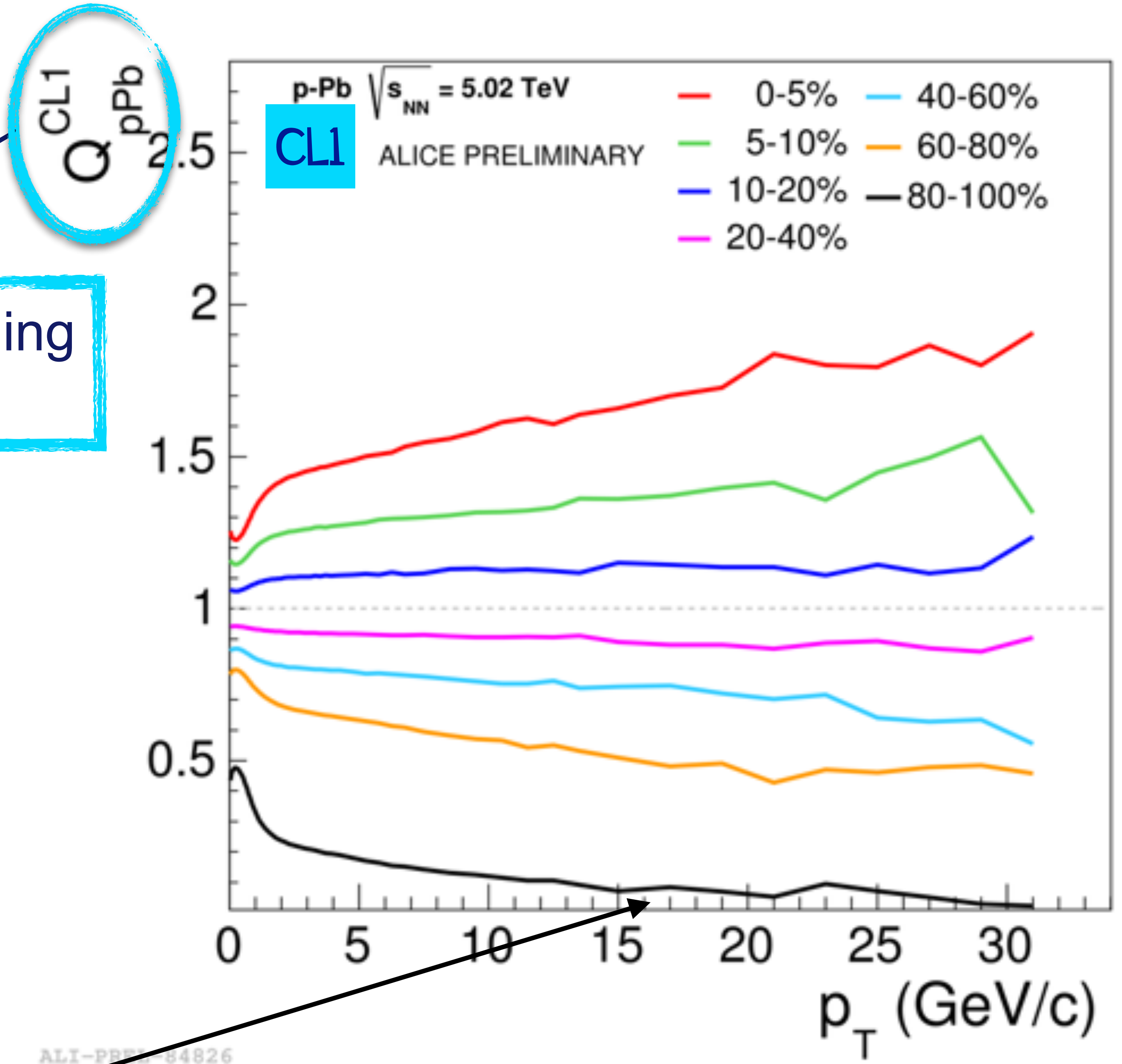

ALICE Coll., Phys. Rev. C 91 (2015) 064905

Jet-veto effect in CL1 most peripheral bin with a significant negative slope vs p_T

Bias at high p_T

Deviations from binary scaling at high p_T expected

- central (enhanced yield ➧ $R_{pA}>1$) and peripheral (lower yield ➧ $R_{pA}<1$) classes

- G-PYTHIA incoherent superposition of NN collisions reproduces the biases!

- $Q_{pPb} = R_{pPb}$ including possible biases

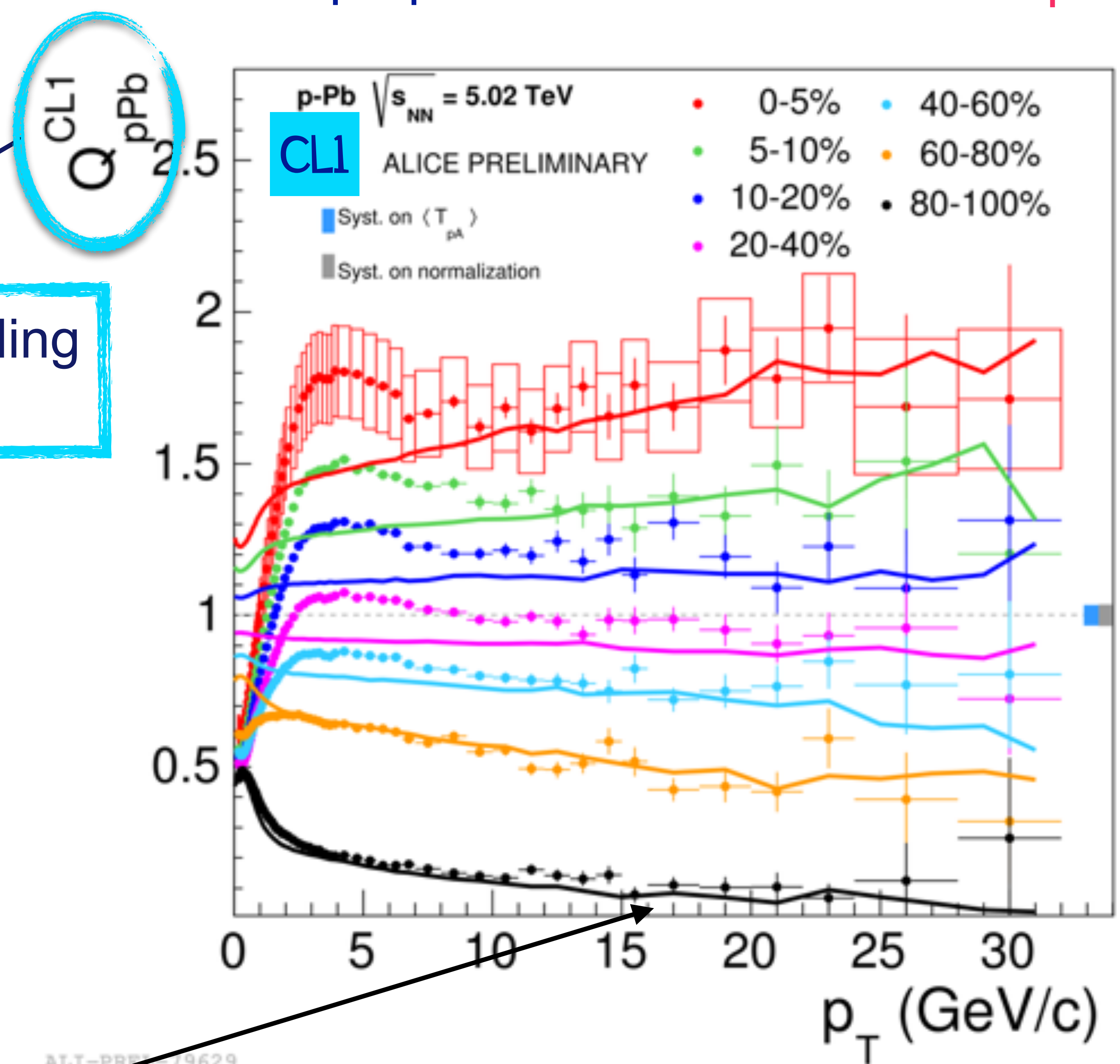

ALICE Coll., Phys. Rev. C 91 (2015) 064905

Jet-veto effect in CL1 most peripheral bin with a significant negative slope vs p_T

Bias vs. rapidity

➧ the bias reduced increasing Δy between the tracking region and the estimator

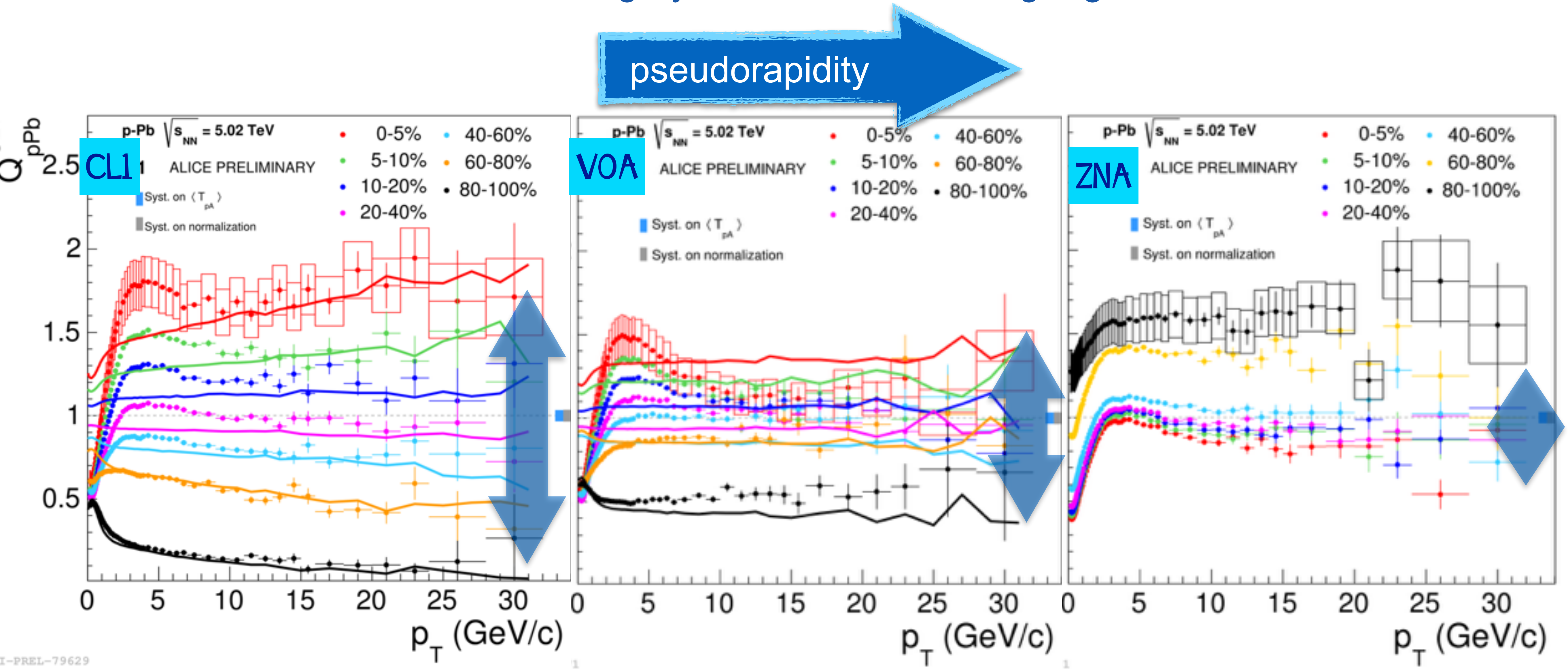

A model to describe Slow Nucleon emission (SNM) is convolved with Glauber to extract $N_{coll}^{Glauber}$ from measured E_{ZN}

SNM is not expected to provide reliable description of peripheral data ➧ the remaining bias in ZNA is NOT due to the event selection but to the unaccurate estimate of N_{coll} provided by the model

Unbiased centrality selection

Assumption ➧ an event selection based on ZN energy does not induce any bias on particle production at smaller rapidities (equivalent to assume that forward nuclear emission is directly related to geometry and not sensitive to hard processes)

Assumptions ➧ based on observed scaling of particle production vs. η:

- charged particle multiplicity @ midrapidity scales with N_{part} (predicted by Wounded Nucleon Model, verified for MB measurement)

$$< N_{coll} >_i^{mult} = < N_{part} >_{MB} \cdot \left(\frac{< dN/d\eta >_i}{< dN/d\eta >_{MB}} \right) - 1$$

- yield of charged high-p_T particle @ midrapidity scales with N_{coll} (valid for MB measurement)

$$< N_{coll} >_i^{highp_T} = < N_{coll} >_{MB} \cdot \frac{< Y_{highp_T} >_i}{< Y_{highp_T} >_{MB}}$$

- target-going particle multiplicity scales as $N_{part}^{Pb} = N_{part} - 1 = N_{coll}$

$$< N_{coll} >_i^{Pb-side} = < N_{coll} >_{MB} \cdot \frac{< Y^{Pb-side} >_i}{< Y^{Pb-side} >_{MB}}$$

Unbiased centrality selection

Assumption ➧ an event selection based on ZN energy does not induce any bias on particle production at smaller rapidities (equivalent to assume that forward nuclear emission is directly related to geometry and not sensitive to hard processes)

ALICE Coll., Phys. Rev. C 91 (2015) 064905

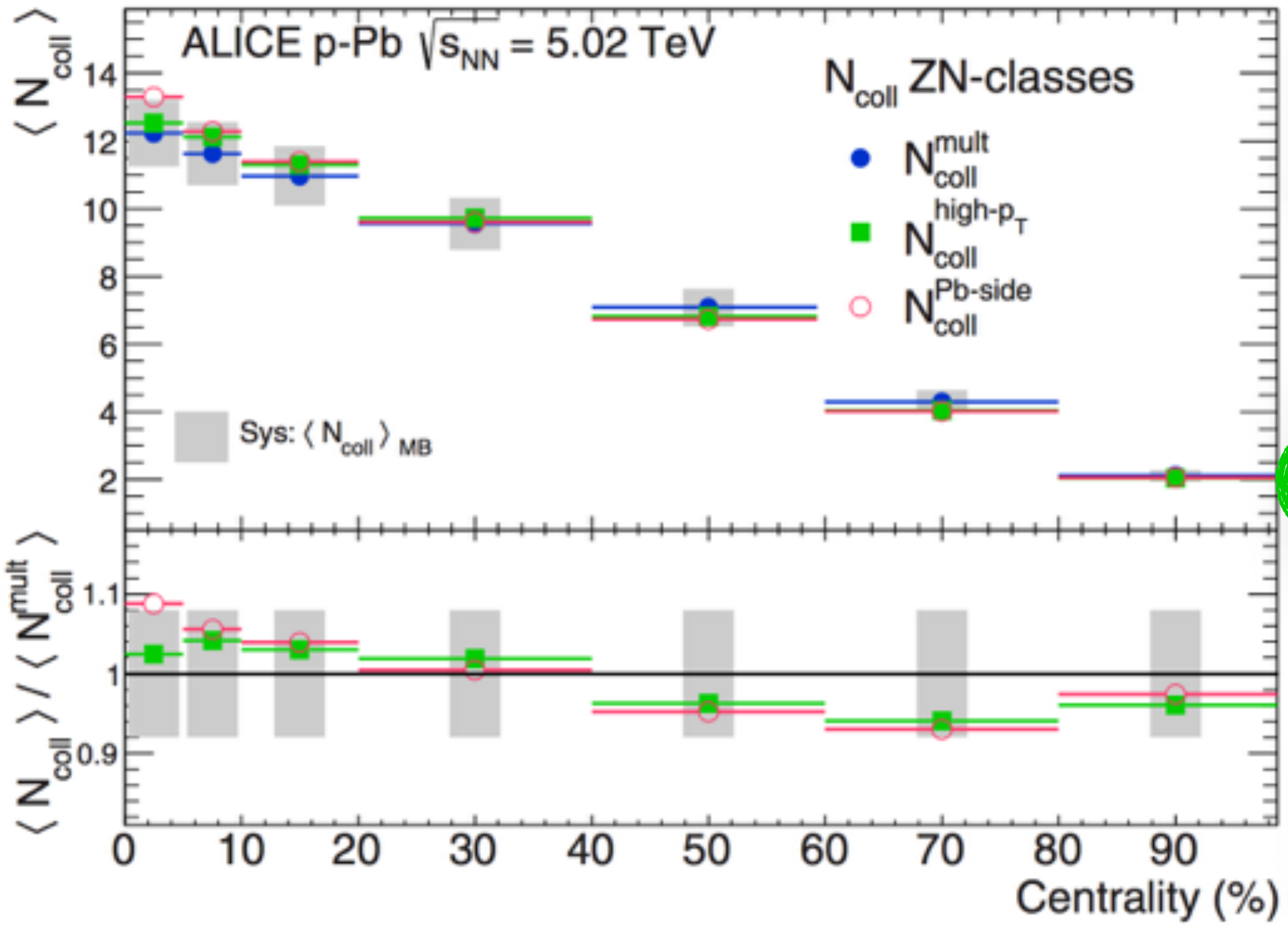

$$< N_{coll} >_i^{mult} = < N_{part} >_{MB} \cdot \left(\frac{< dN/d\eta >_i}{< dN/d\eta >_{MB}} \right) - 1$$

$$< N_{coll} >_i^{highp_T} = < N_{coll} >_{MB} \cdot \frac{< Y_{highp_T} >_i}{< Y_{highp_T} >_{MB}}$$

$$< N_{coll} >_i^{Pb-side} = < N_{coll} >_{MB} \cdot \frac{< Y^{Pb-side} >_i}{< Y^{Pb-side} >_{MB}}$$

➧ consistency of the 3 assumptions within 10%

dN/dη

ALICE Coll., Phys. Rev. C 91 (2015) 064905

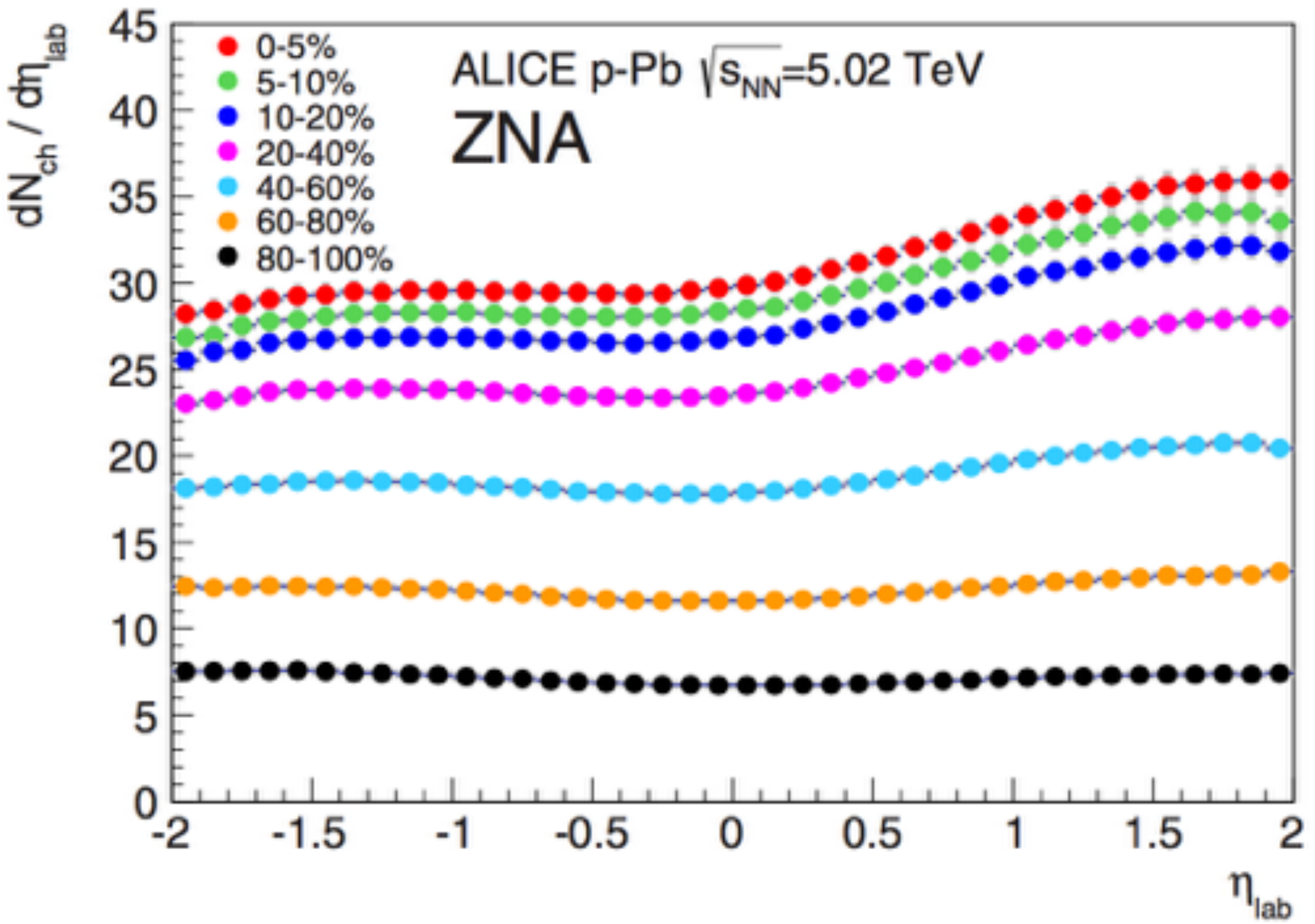

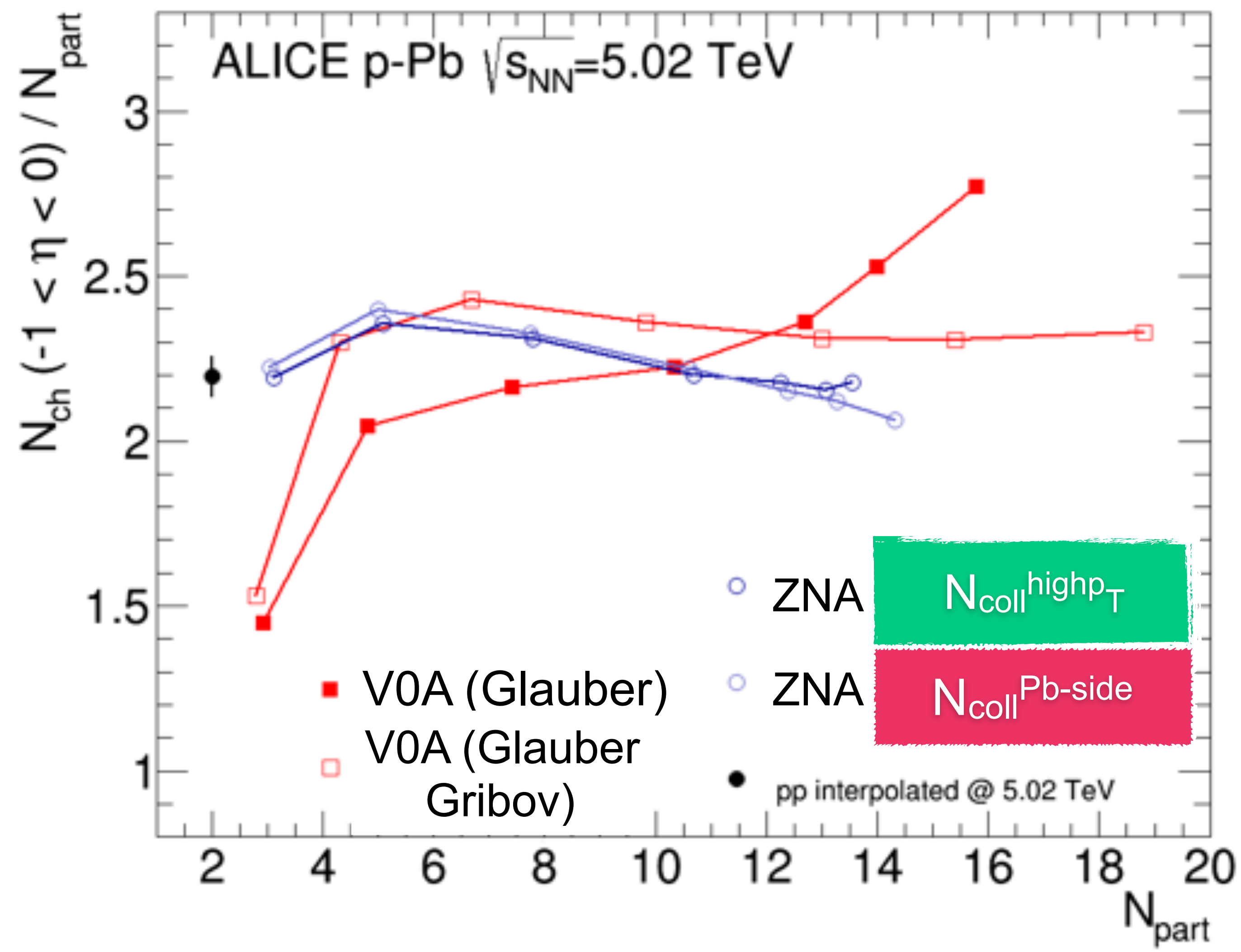

- V0A Glauber fit: steeper than linear increase in N_{part}
- V0A Glauber-Gribov fit: ~ linear scaling with N_{part} apart from most peripheral bin

- ZN centrality + N_{coll} from high-p_T and Pb-fragmentation side assumption: linear scaling with N_{part} (within 10%) and the most peripheral bin in agreement with pp data

Nuclear modification factor

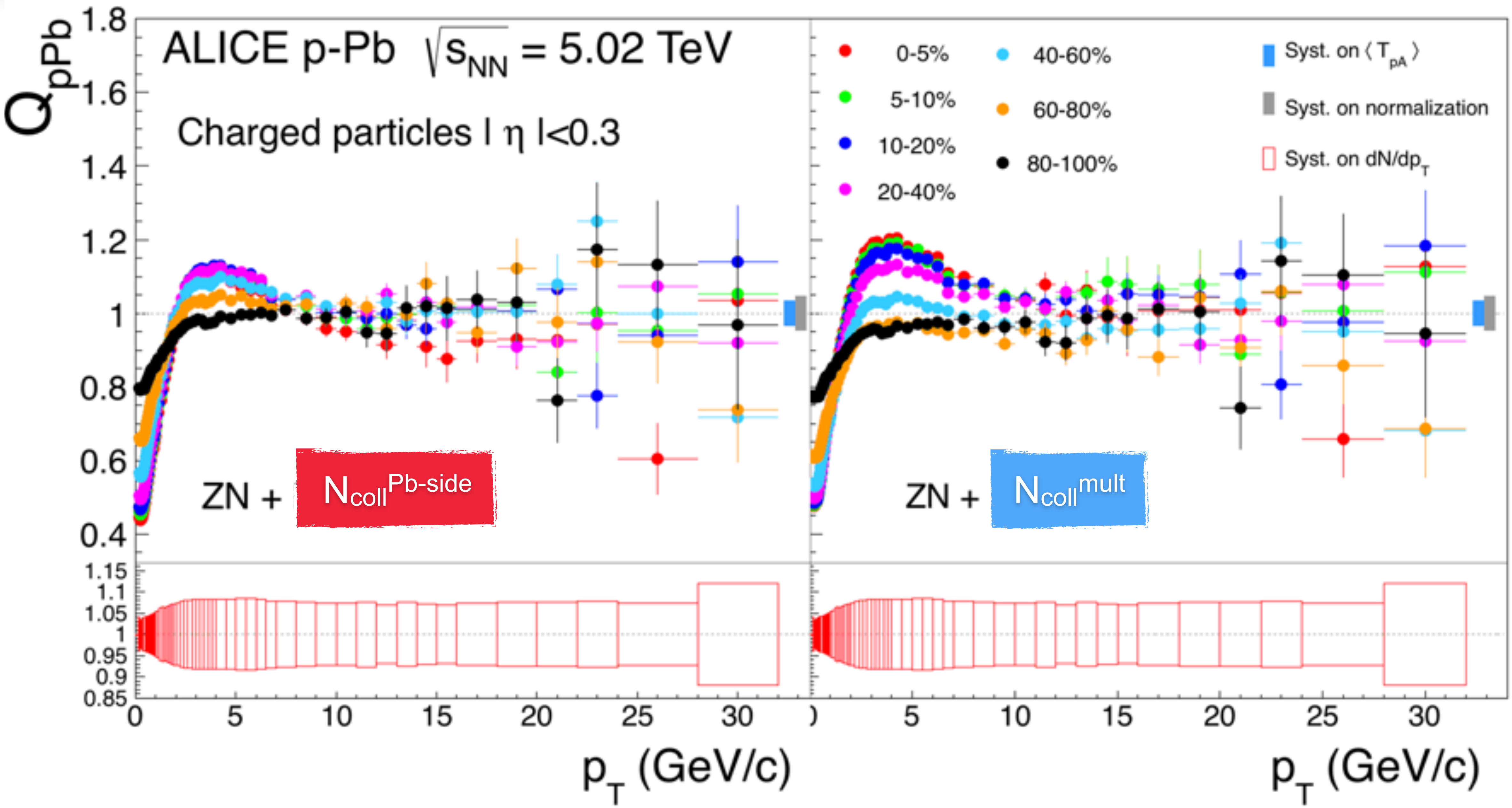

ALICE Coll., Phys. Rev. C 91 (2015) 064905

Nuclear modification factors ➧ @ high p_T the yield is consistent with binary scaling over the whole centrality range

➧ Results from the 2 assumptions are in agreement within uncertainties

Yield at high p_T

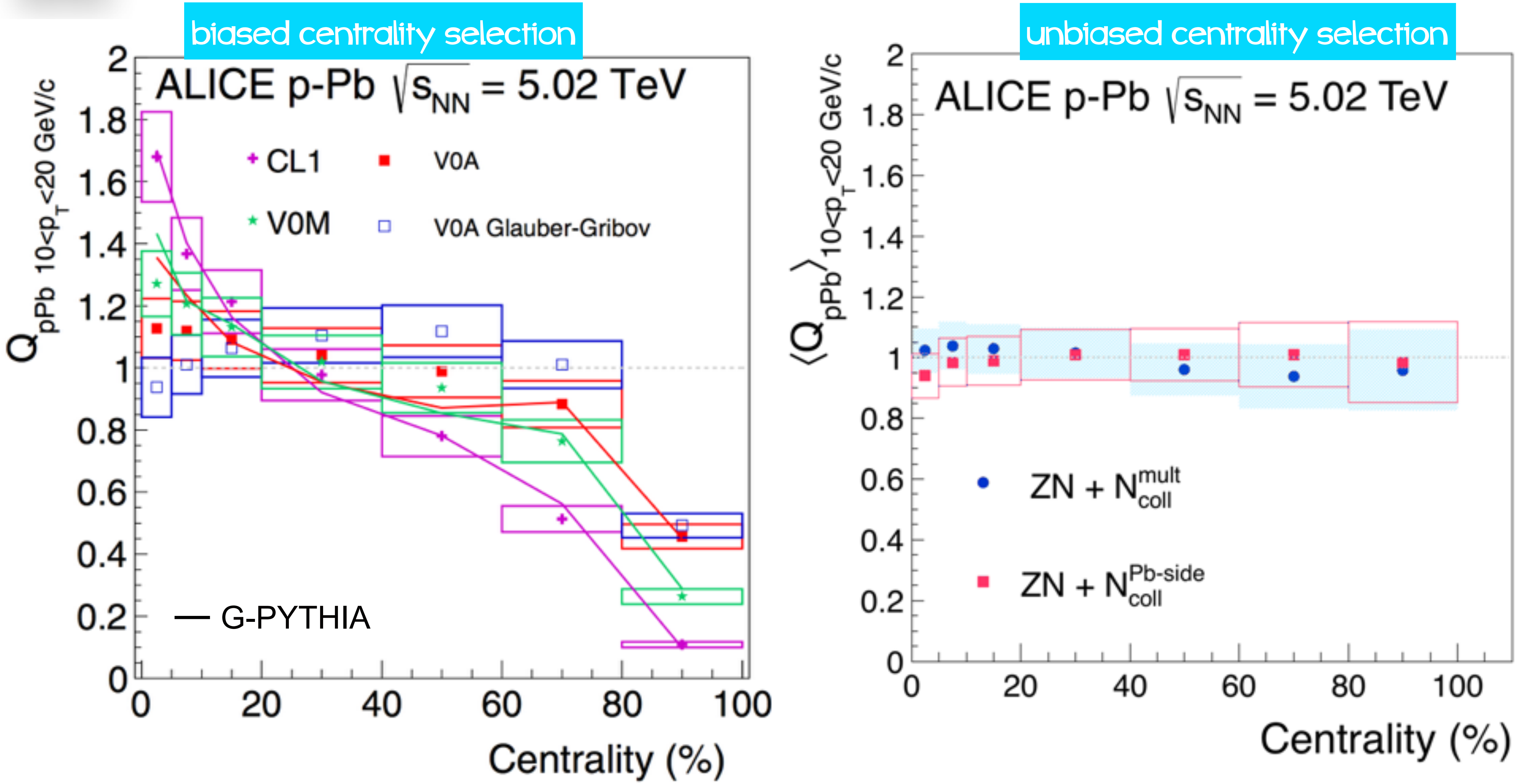

ALICE Coll., Phys. Rev. C 91 (2015) 064905

Centrality selection based on multiplicity ➧ bias at high p_T over the whole centrality range

ZN centrality selection + assumptions on dN/dη, Pb-side ➧ no centrality dependence and binary scaling for high-p_T yields

Two-particle correlations

ALICE Coll., PLB 719 (2013) 29

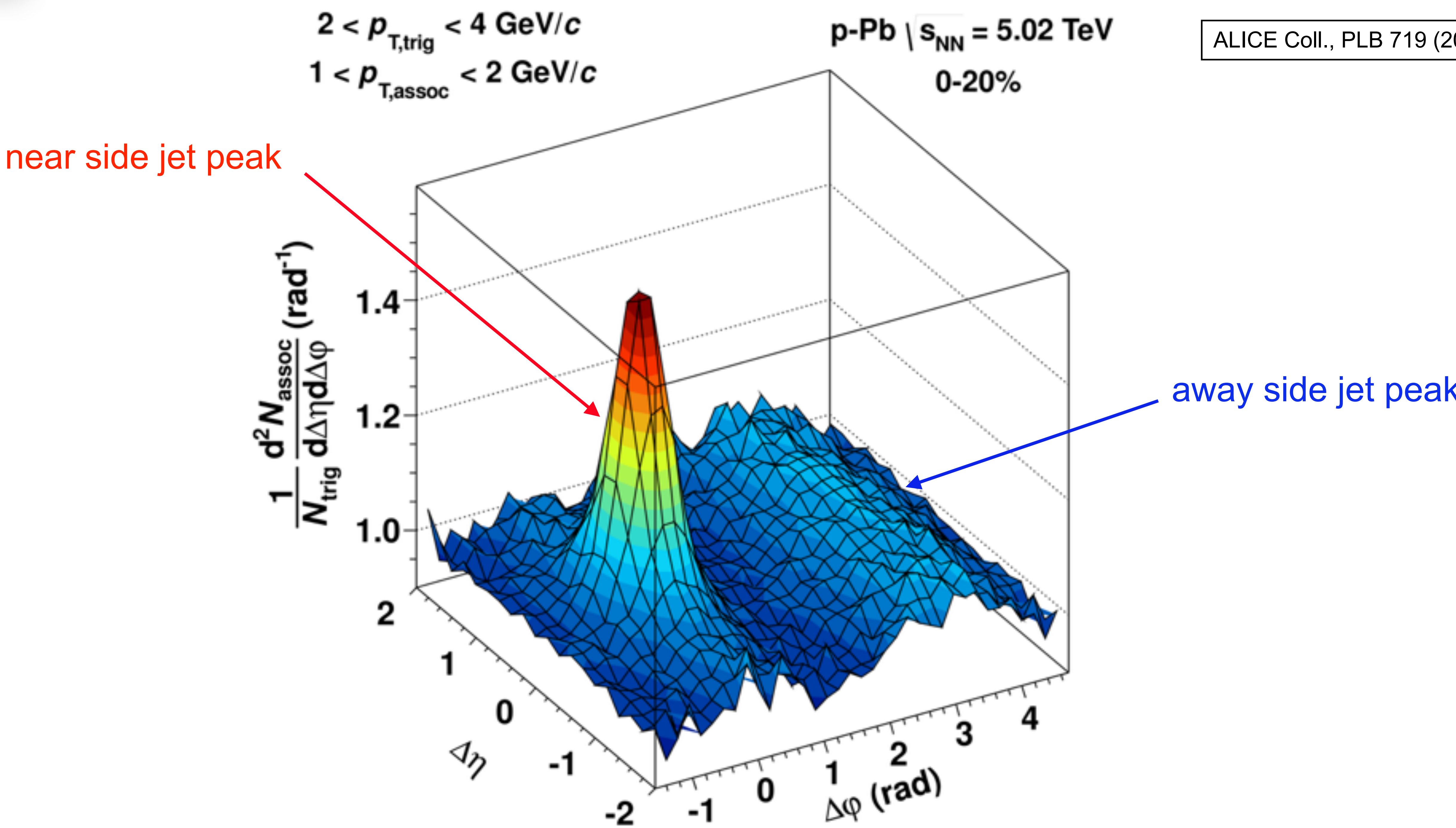

- subtract jet contribution to study Long Range Correlations
- subtract long range correlations to study jet-like short range correlations

Jet-like correlations

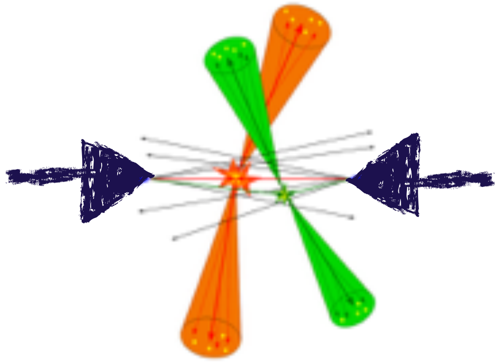

Minijets produced in hard scattering events
Overlapping minijets produced in high multiplicity events are interpreted as due to MPIs
➧ studied on statistical basis to probe MPIs

➧ Two-particle azimuthal correlations
Measure Δφ between pairs of TRIGGER and ASSOCIATED particles at low p_T
Nearside (NS) Δφ~0 and awayside (AS) Δφ~π yields provide information about the fragmenting properties of the partons producing the jets

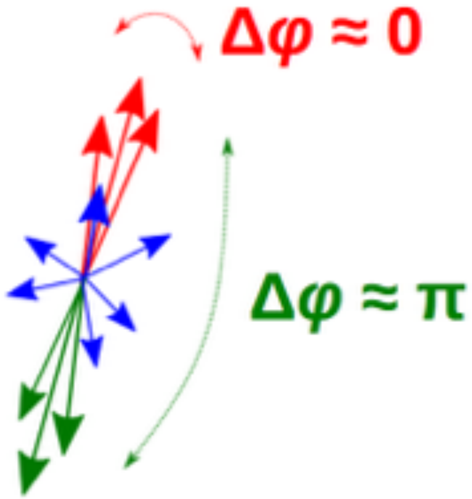

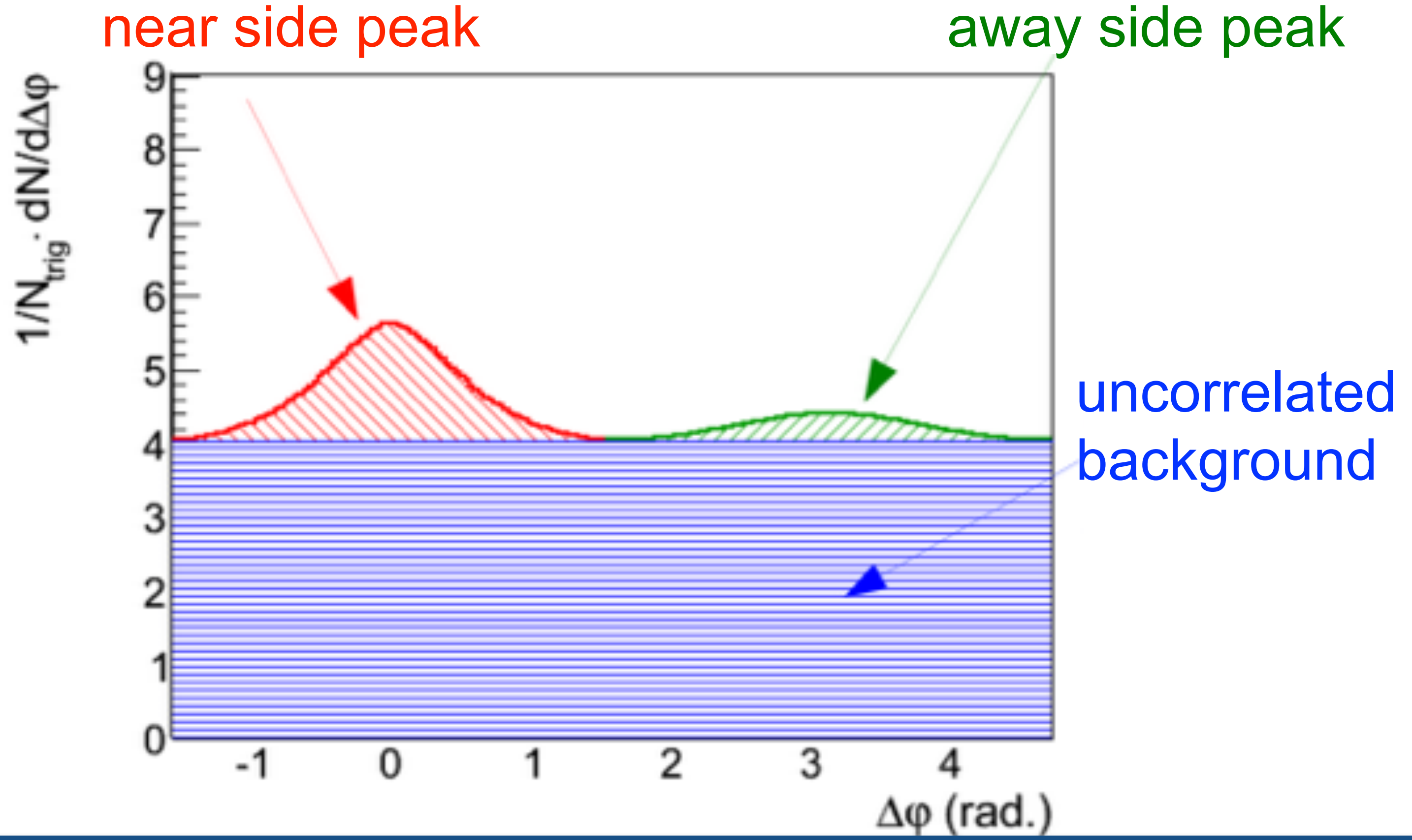

Observables

Observables ➧ per trigger yields in NS $N_{\text{assoc, nearside}}$ and AS $N_{\text{assoc, awayside}}$ peaks, $N_{\text{uncorrelated seeds}}$

$$\langle N_{\text{uncorrelated seeds}} \rangle = \frac{\langle N_{\text{trig}} \rangle}{\langle N_{\text{correlated triggers}} \rangle} = \frac{\langle N_{\text{trig}} \rangle}{\langle N_{\text{assoc,nearside}} \rangle + \langle N_{\text{assoc,awayside}} \rangle + 1}$$

➧ $N_{\text{uncorrelated seeds}}$ provides the number of independent sources of particle production and contains information about the number of semi-hard scatterings in the events

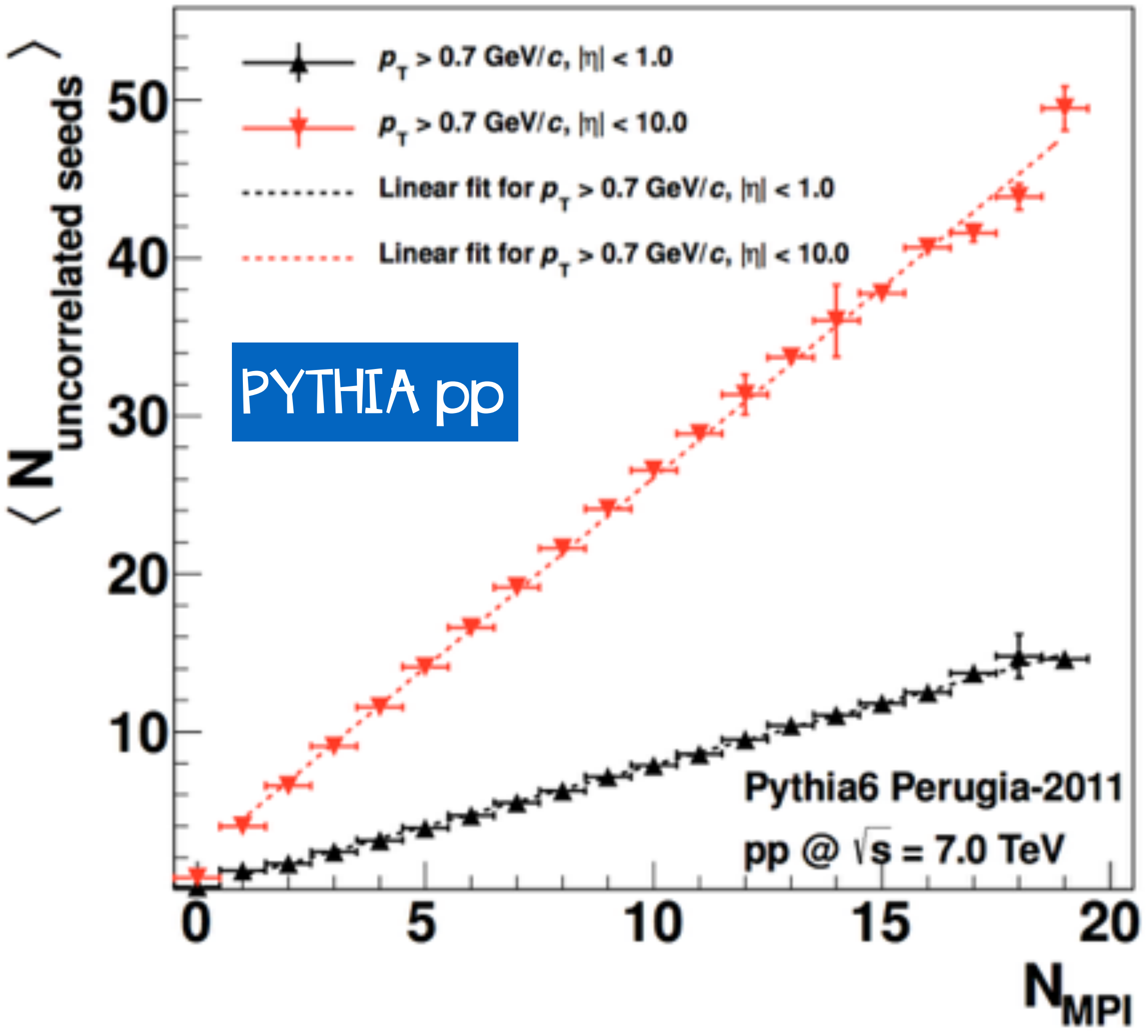

➧ PYTHIA predicts a strong correlation between uncorrelated seeds and MPIs

Nearside yield

- sensitive to jet fragmentation properties (of low p_T leading particles)

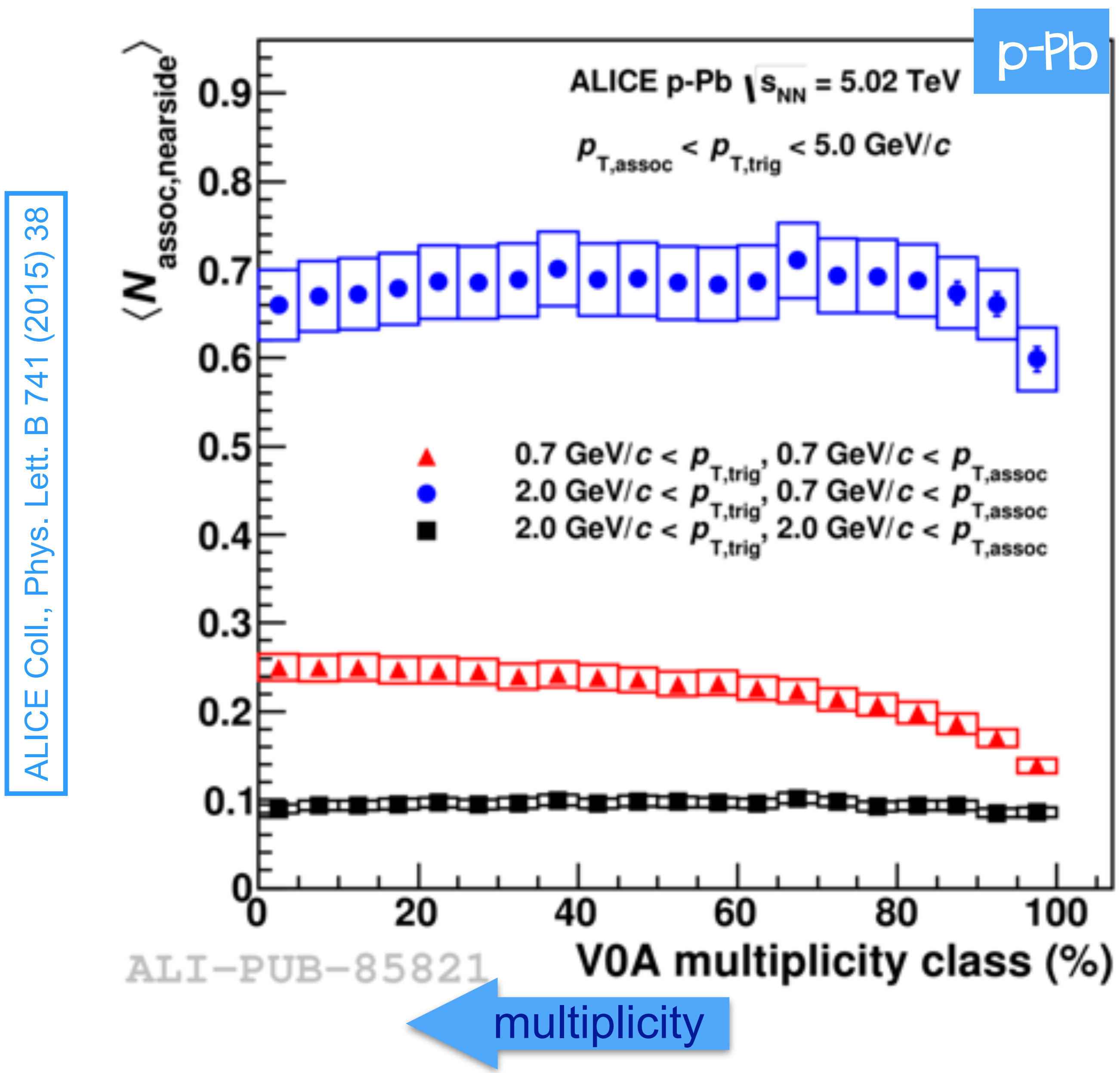

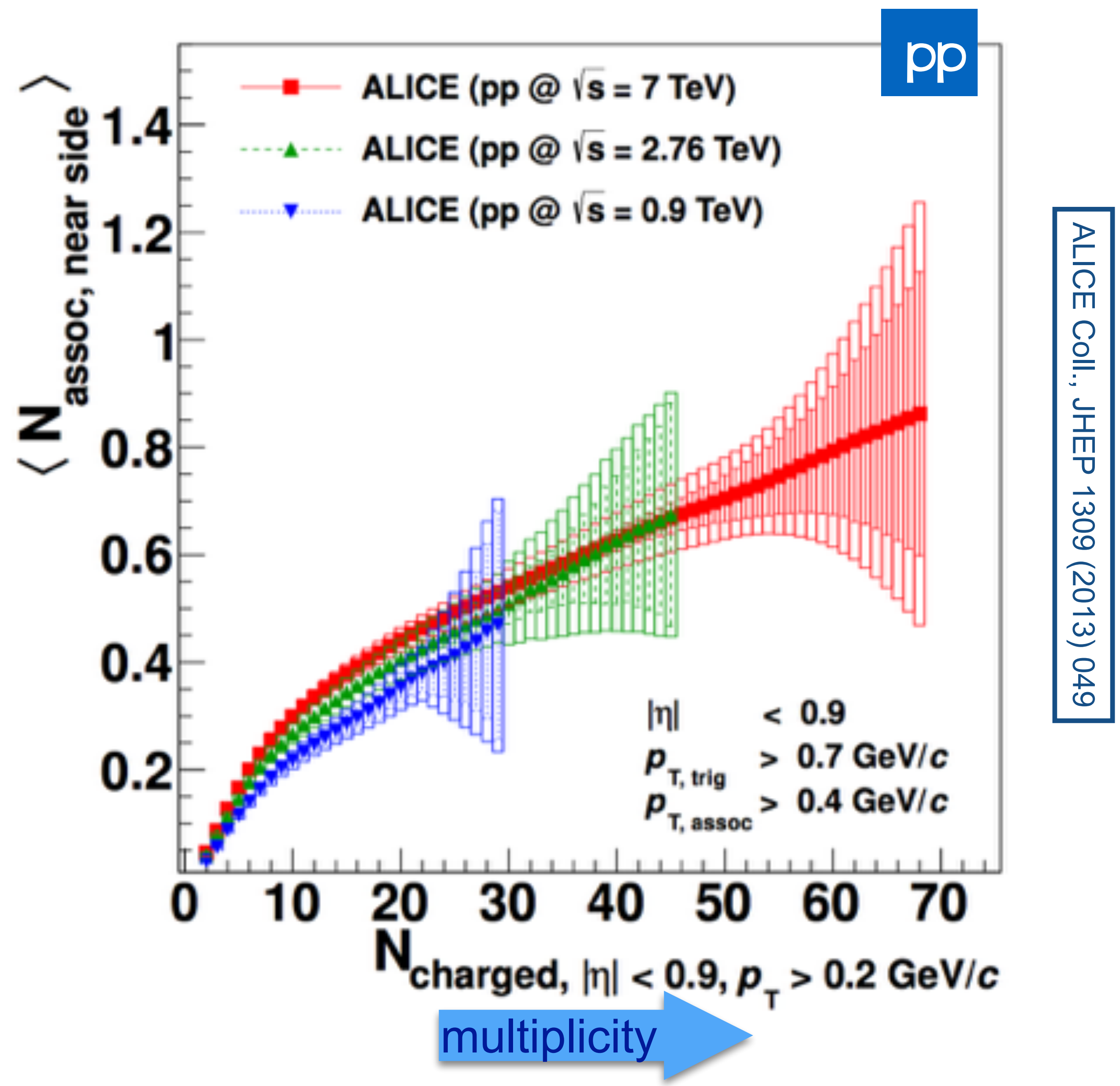

- high multiplicity events have the same number of associated yield per trigger particle in jet peak
- consistently with incoherent fragmentation of multiple-parton scatterings

Awayside yield

- sensitive to jet fragmentation properties (for low p_T recoil particles)

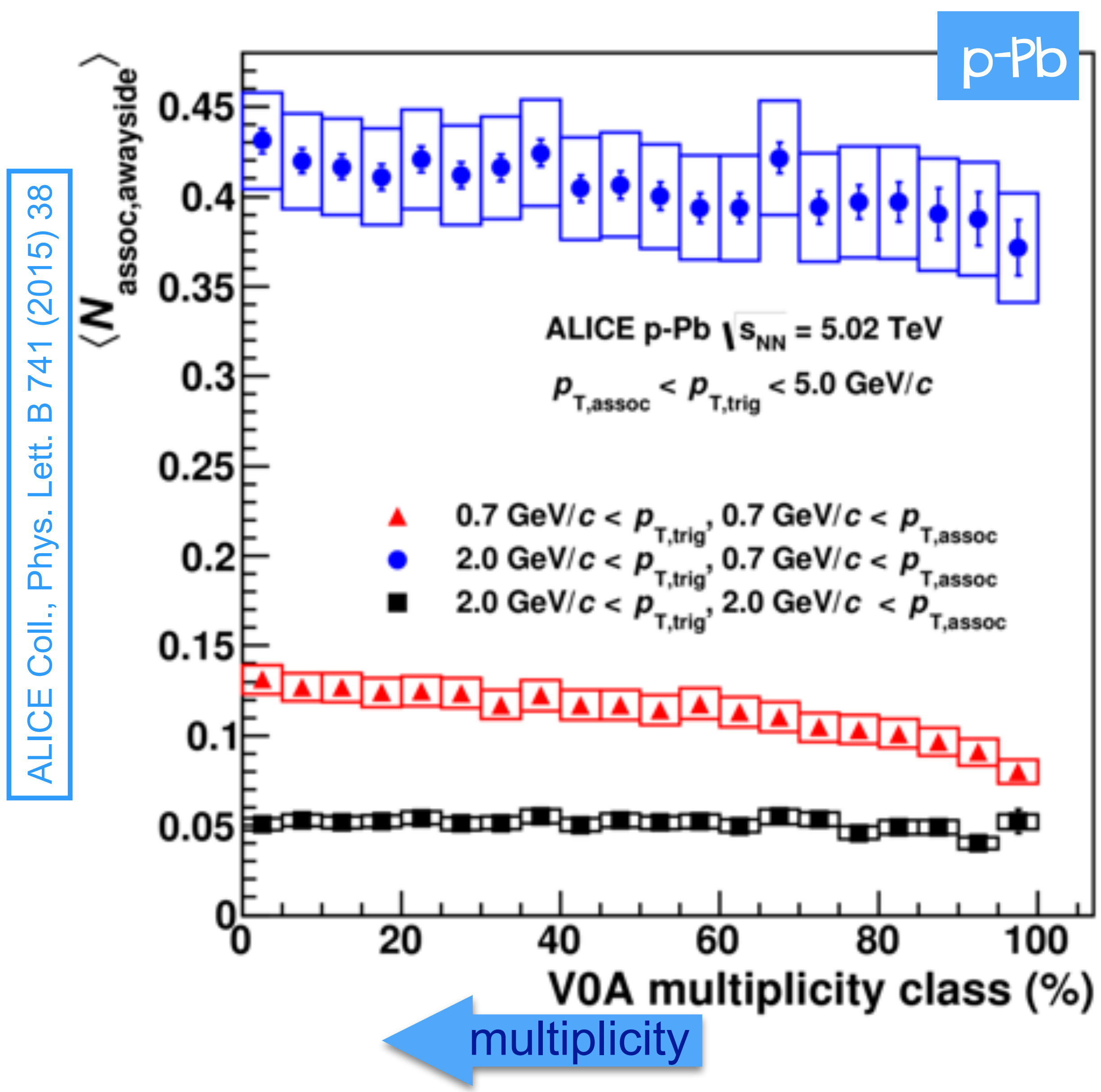

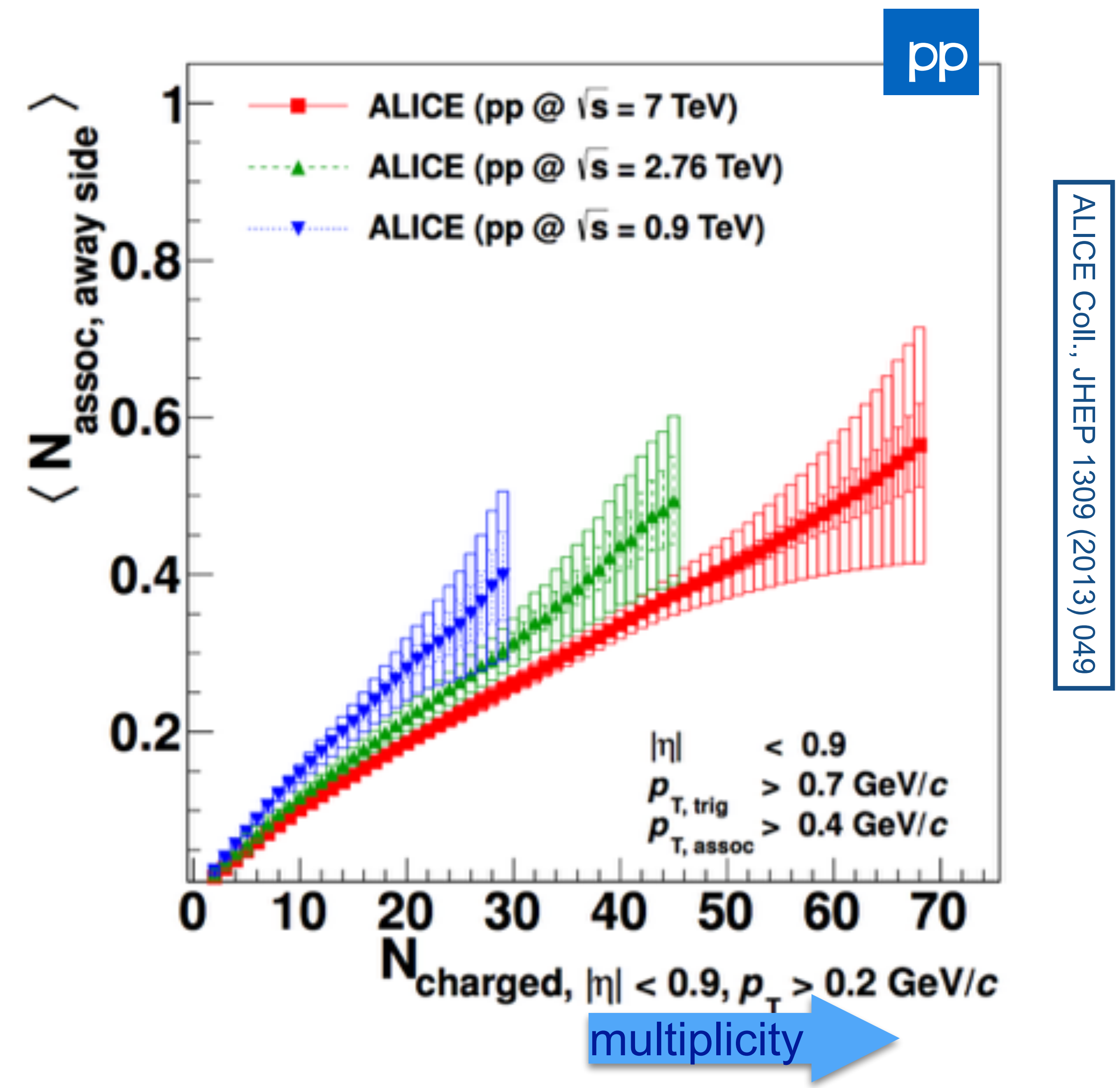

- high multiplicity events are not built by a higher number of particles in recoiling jet peak
- absence of coherence effects for large number of MPIs in p-Pb collisions

Uncorrelated seeds

- Uncorrelated seeds to probe the number of semi-hard scatterings

ALICE Coll., Phys. Lett. B 741 (2015) 38

p-Pb

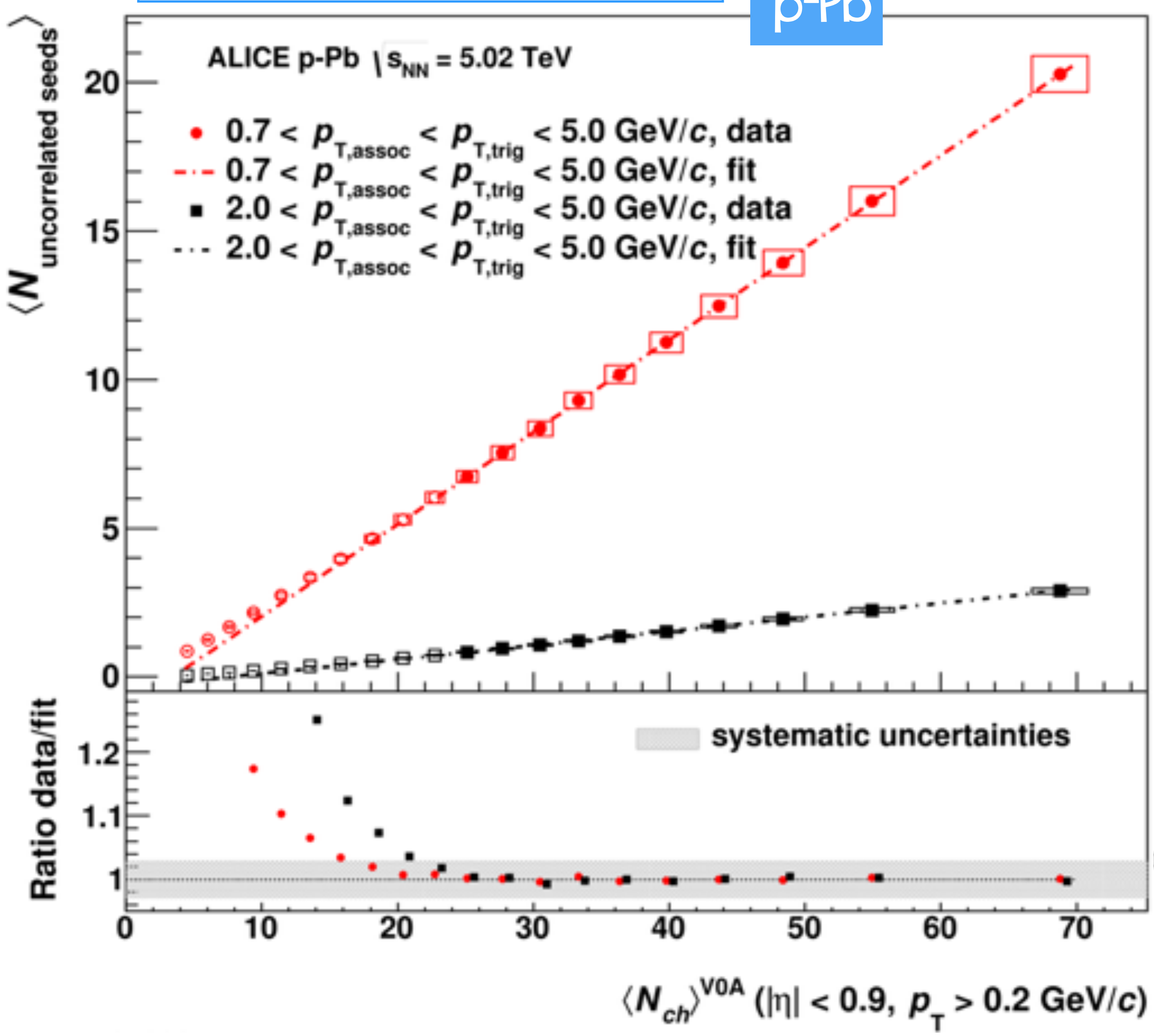

ALICE Coll., JHEP 1309 (2013) 049

pp

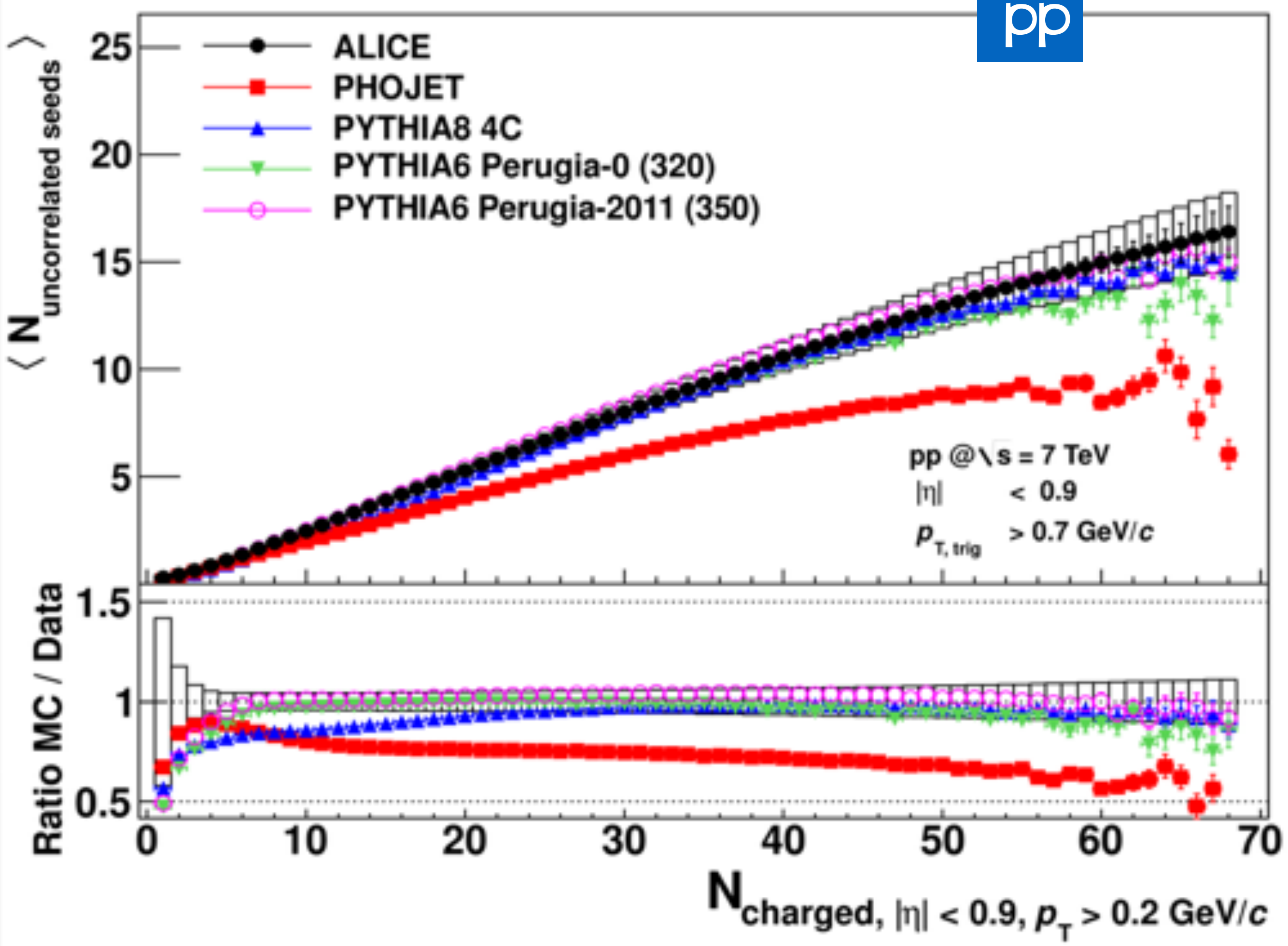

- $N_{uncorrelated\ seeds}$ increases with particle multiplicity
- In p-Pb MPIs scale linearly with $N_{charged}$ while in pp there is an indication of a saturation in number of parton-parton interactions

Uncorrelated seeds

ALICE Coll., Phys. Lett. B 741 (2015) 38

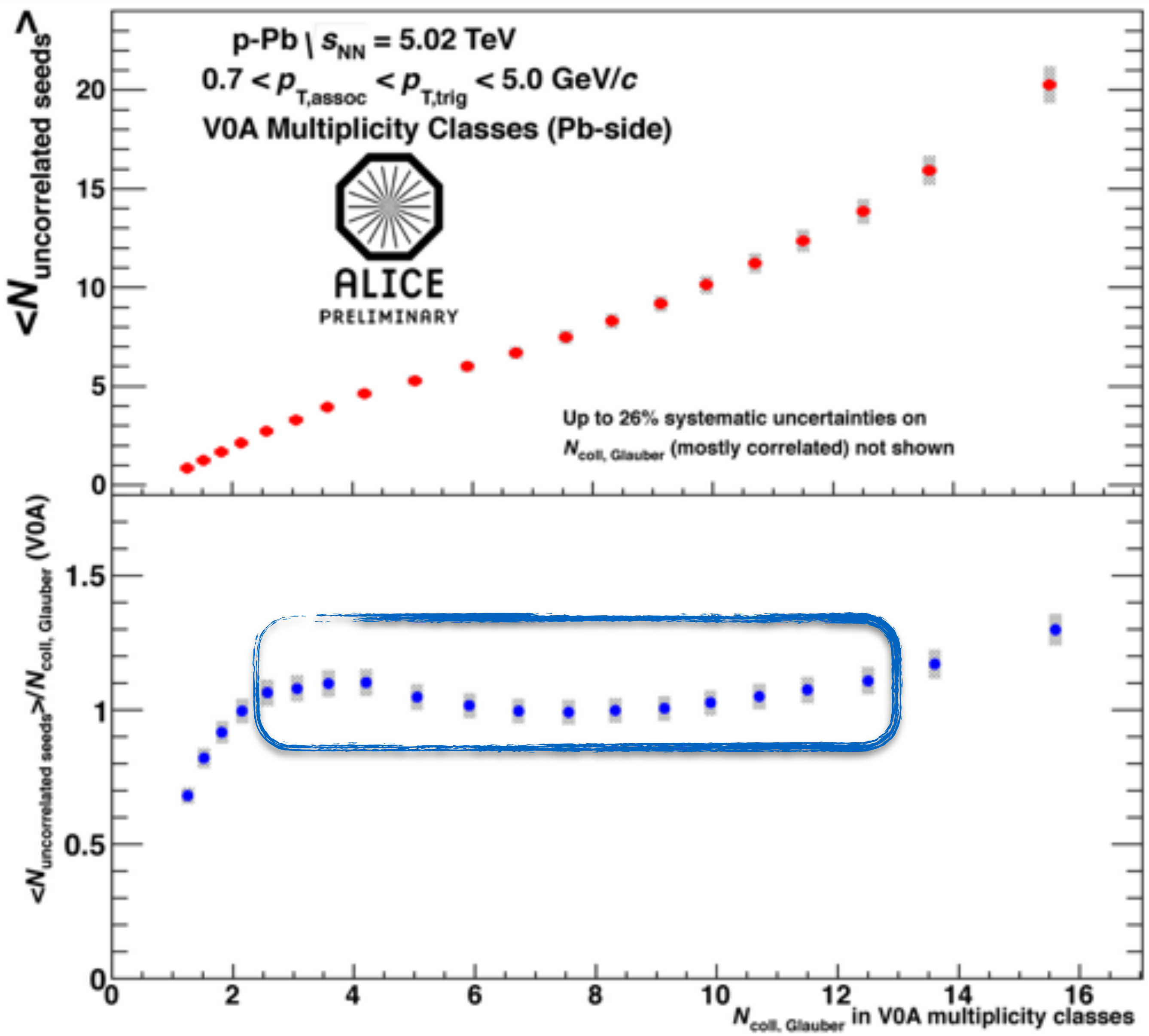

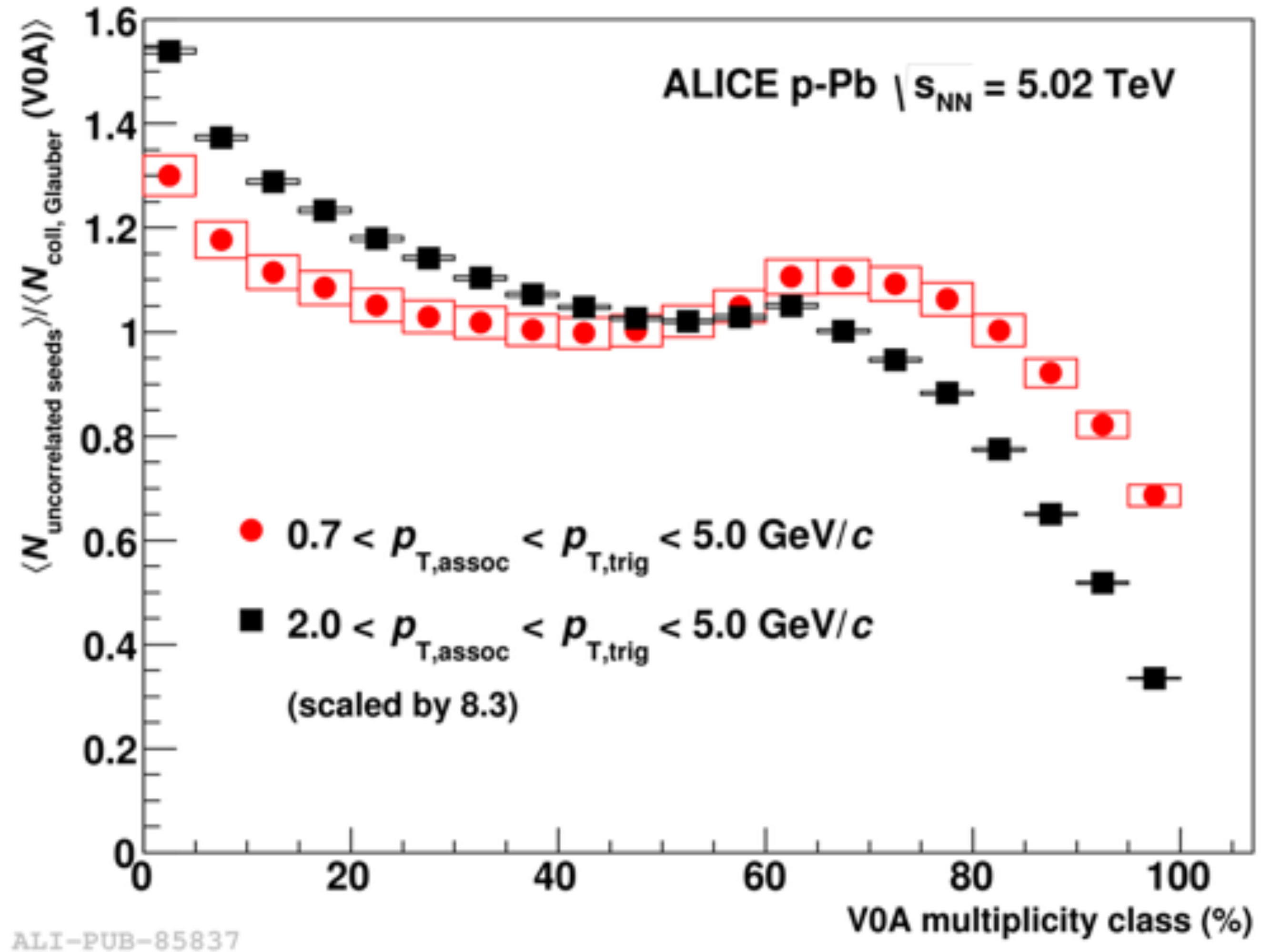

$N_{\text{uncorrelated seeds}}$ scales with $N_{\text{coll Glauber}}$ at intermediate multiplicity: deviations for low and high $N_{\text{coll Glauber}}$ ➧ less/more semi-hard scatterings per p-N collision?
➧ reminds of multiplicity bias!

Uncorrelated seeds

ALICE Coll., Phys. Lett. B 741 (2015) 38

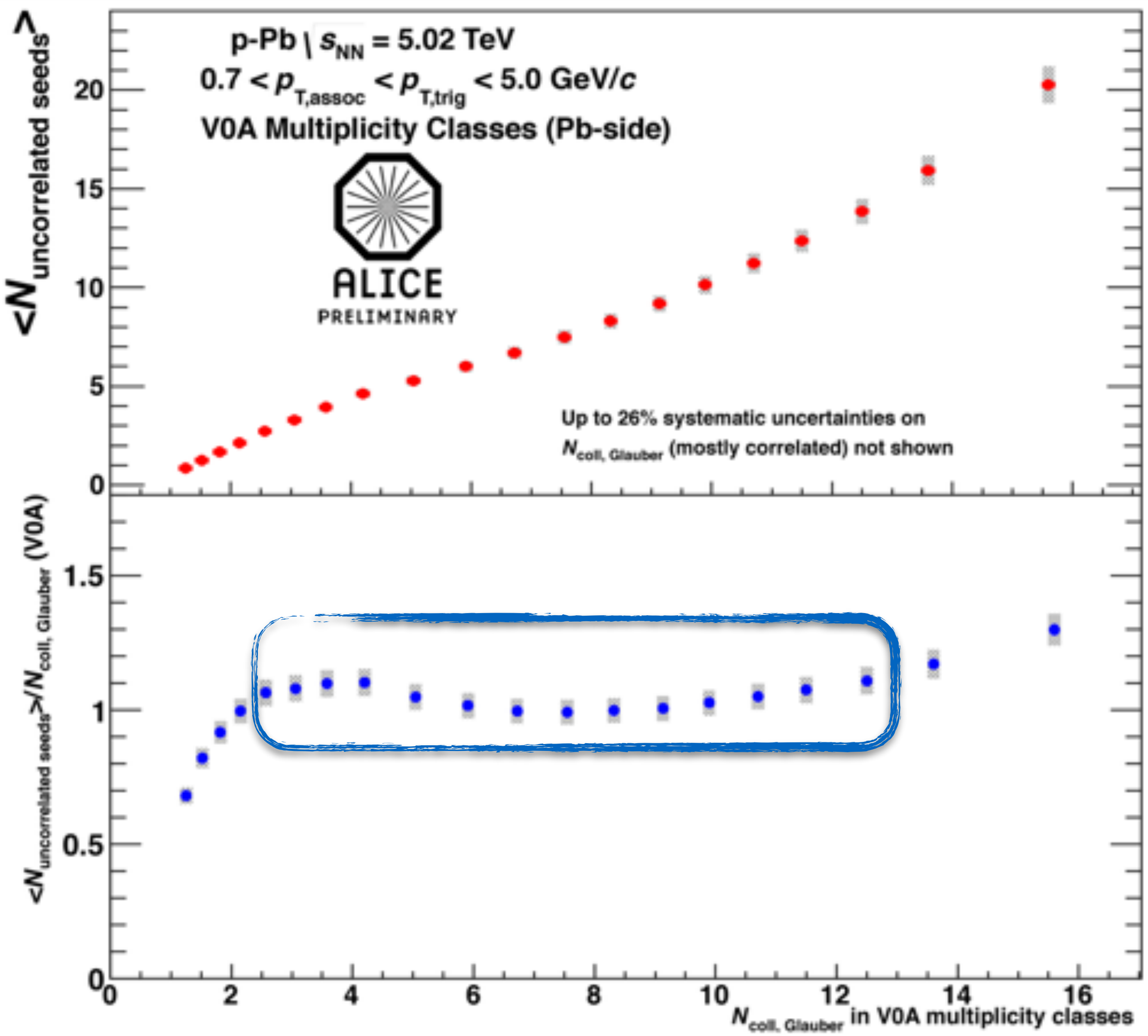

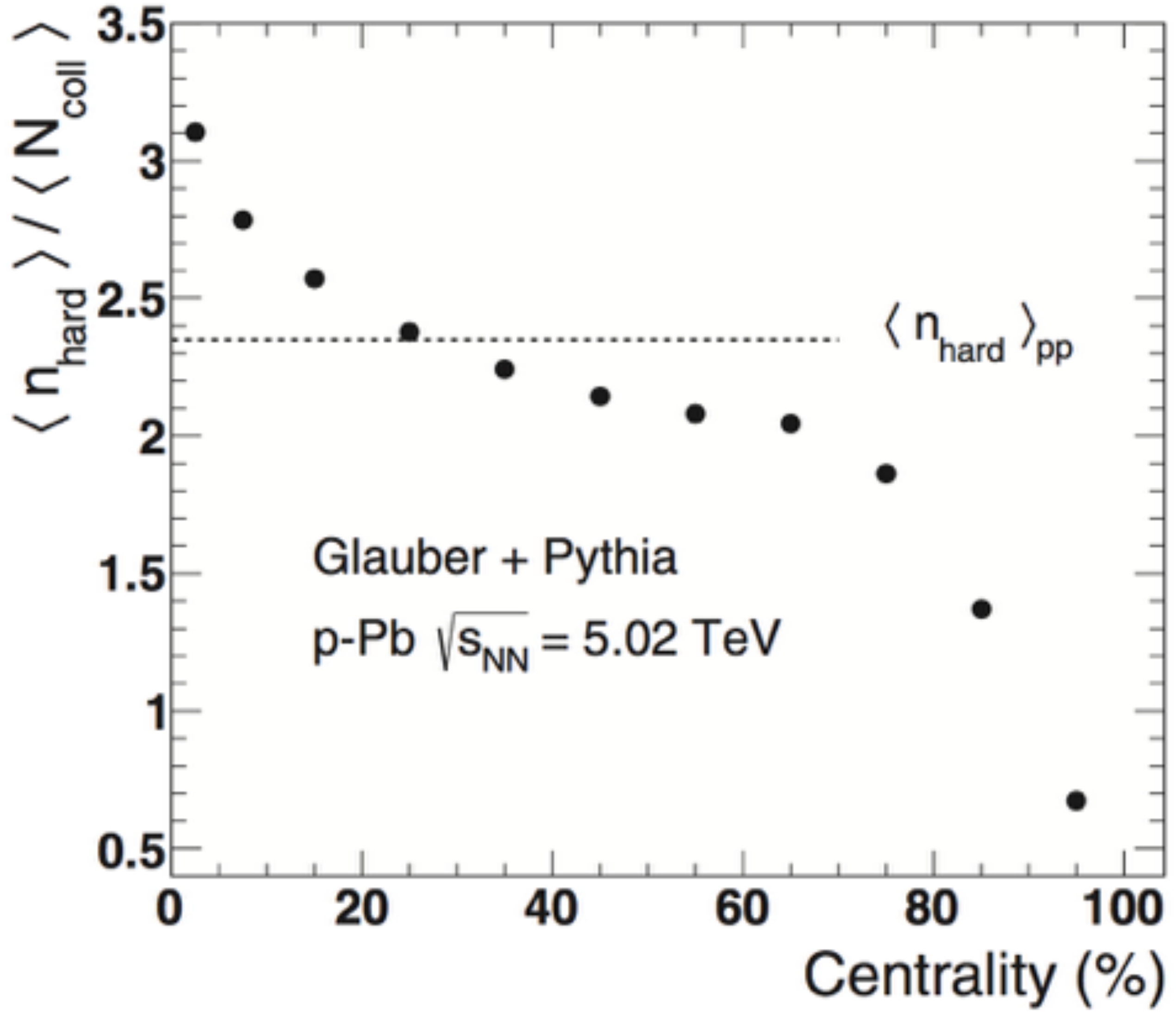

$N_{uncorrelated\ seeds}$ scales with $N_{coll\ Glauber}$ at intermediate multiplicity: deviations for low and high $N_{coll\ Glauber}$ ➧ less/more semi-hard scatterings per p-N collision?
➧ reminds of multiplicity bias!

Emerging picture for p-Pb

ALICE Phys.Lett. B727 (2013) 371-380

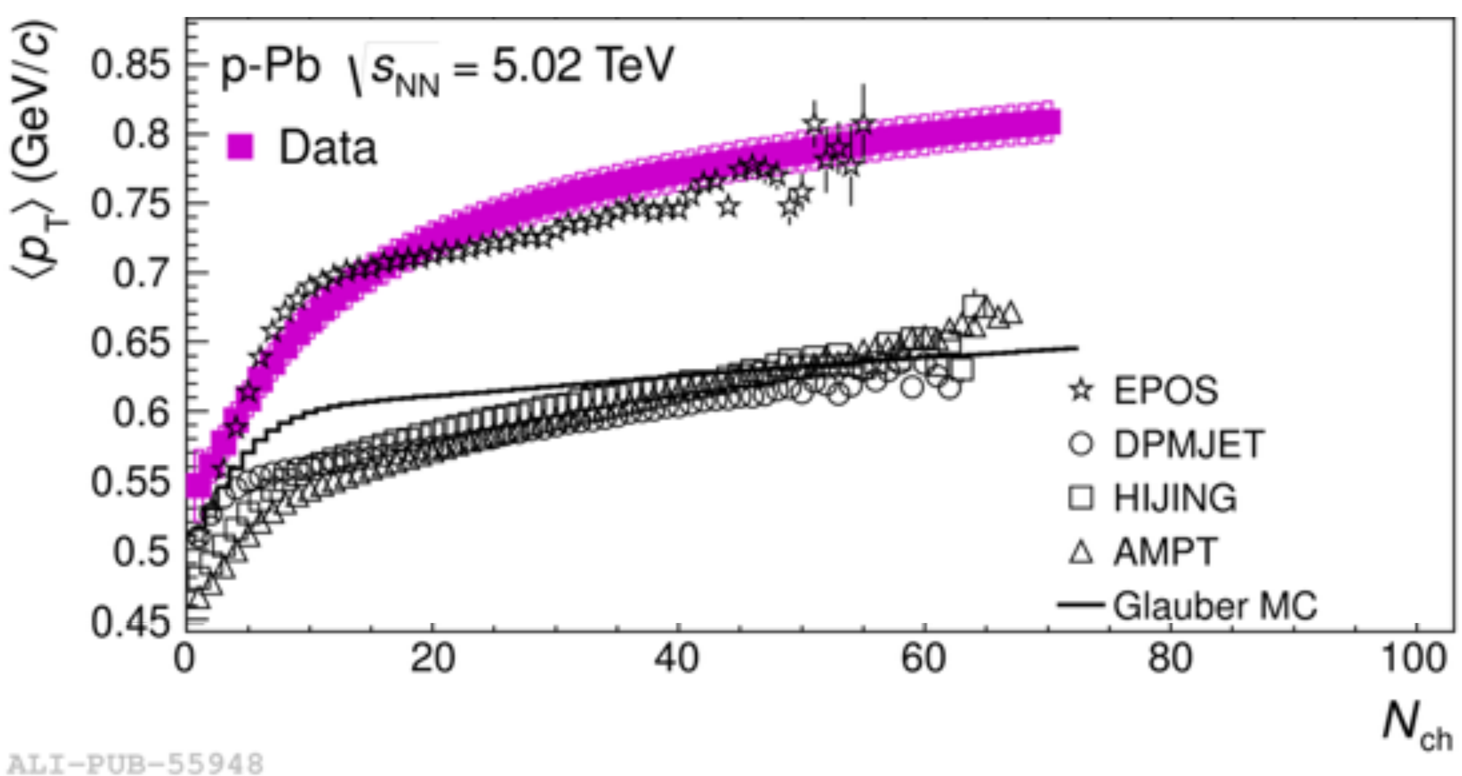

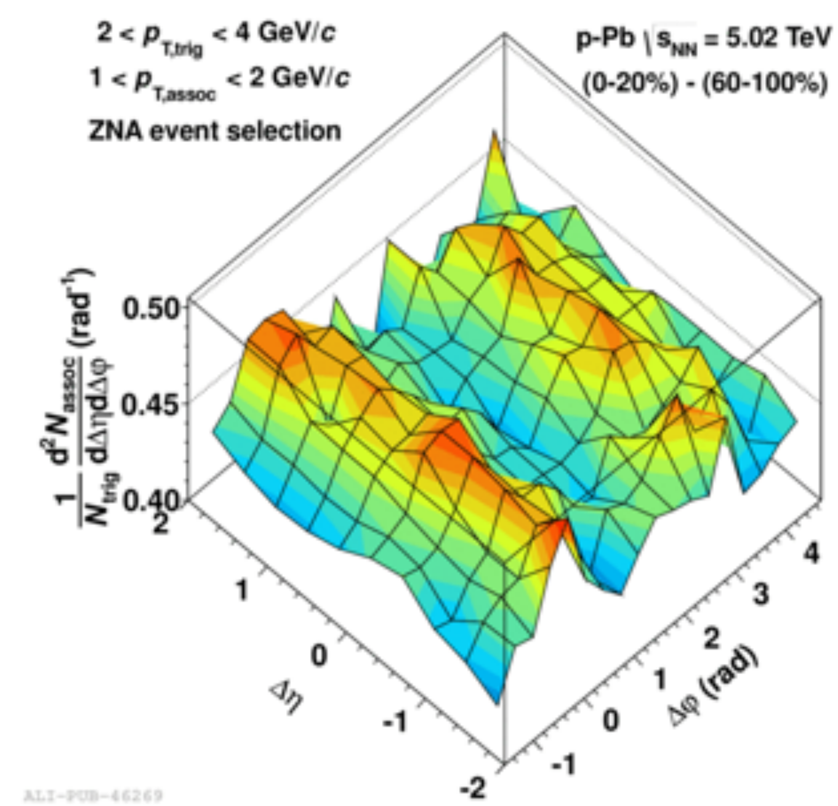

ALICE Coll., PLB 719 (2013) 29

- rise of <p_T> vs. multiplicity and long range correlation results needs coherent effects to be reproduced

- BUT yield per trigger particle in jet-like correlations are unmodified over a wide centrality range, showing no coherence effect for large MPI

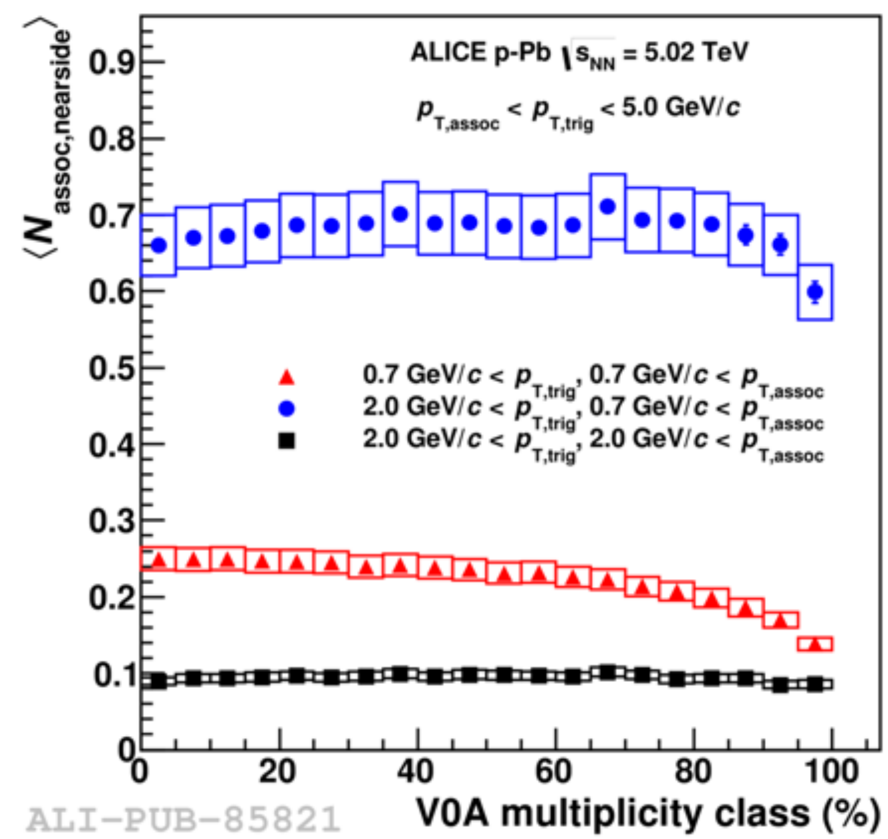

ALICE Coll., Phys. Lett. B 741 (2015) 38

Summary

Insight into Multiple Parton Interactions in p-Pb through:

- centrality selection
- two-particle jet-like correlations

- Bias on centrality selection based on multiplicity estimators
- Multiplicity bias observed in p-A corresponds to a bias in MPIs
- Bias is reduced by increasing y separation between measurement and centrality estimator
- ZN energy provides unbiased centrality selection

- Jet-like angular correlations at low p_T do not show sign of coherent fragmentation effects ➧ constraint for models!
- Uncorrelated seeds (probe for MPIs) scale linearly with unbiased N_{coll}

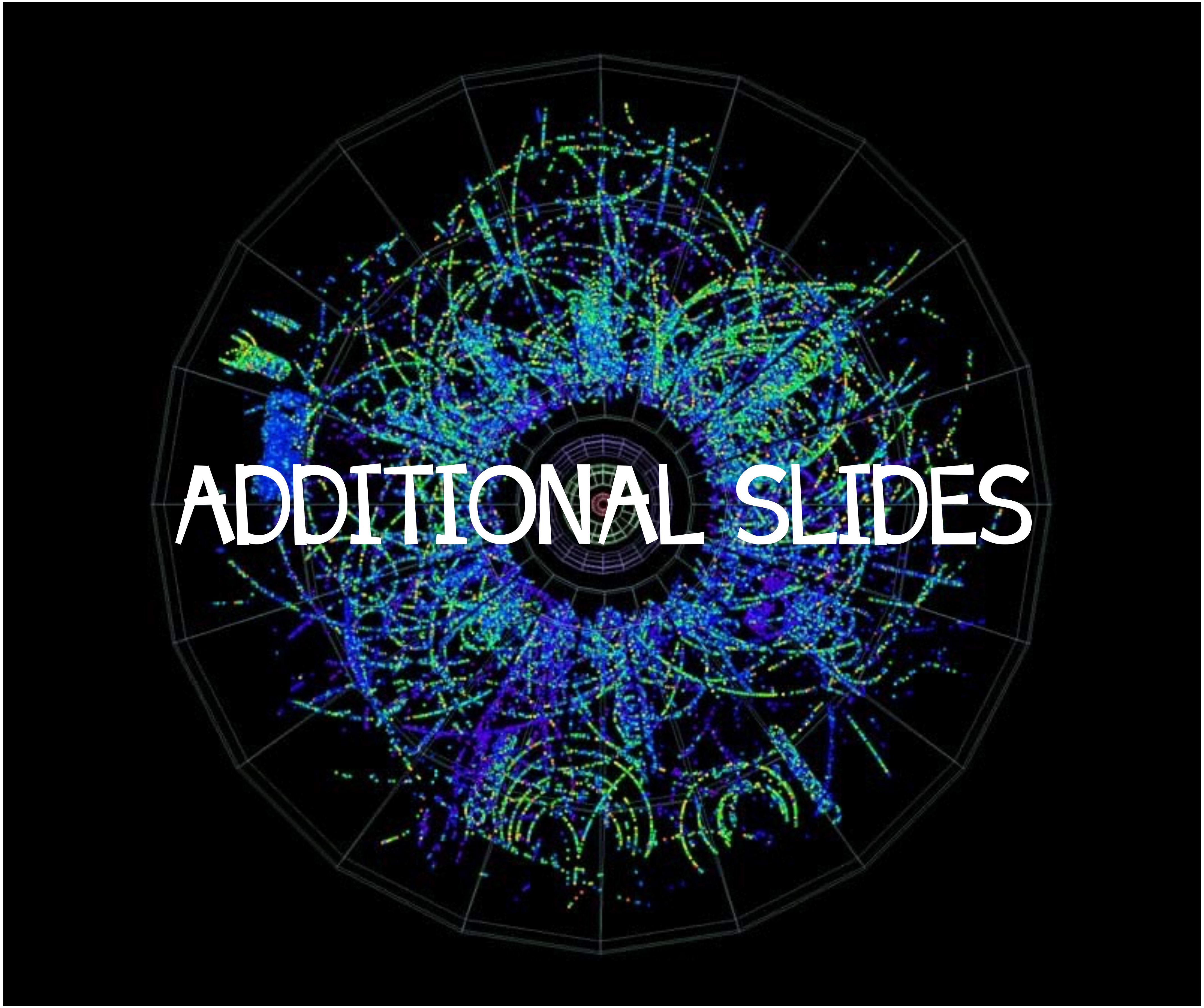
ADDITIONAL SLIDES

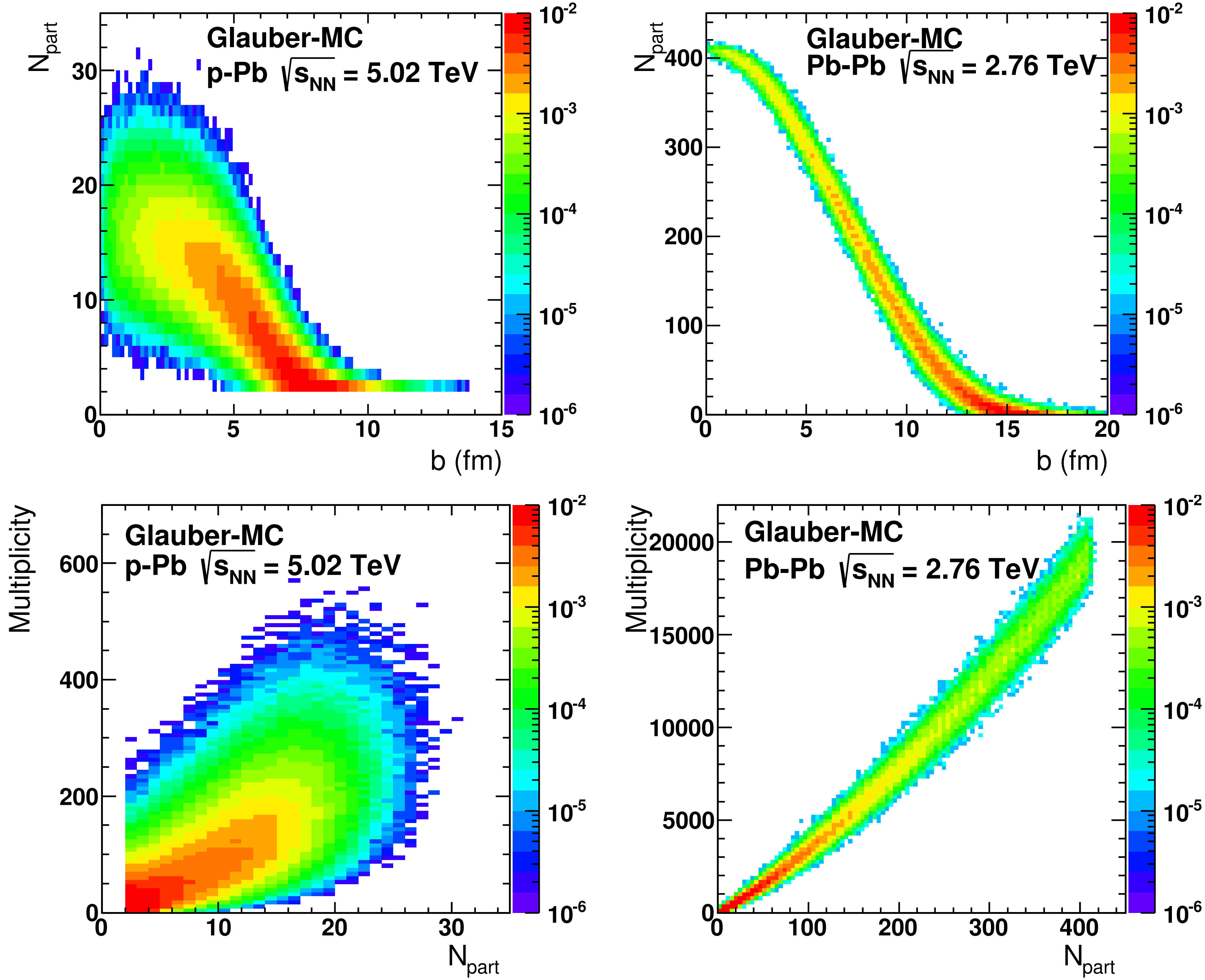
Glauber-MC
p-Pb $\sqrt{s_{NN}}$ = 5.02 TeV
N_{part}
b (fm)
Glauber-MC
Pb-Pb $\sqrt{s_{NN}}$ = 2.76 TeV
N_{part}
b (fm)
Glauber-MC
p-Pb $\sqrt{s_{NN}}$ = 5.02 TeV
Multiplicity
N_{part}
Glauber-MC
Pb-Pb $\sqrt{s_{NN}}$ = 2.76 TeV
Multiplicity
N_{part}

Glauber + NBD fit

Glauber MC + NBD for particle production

- assume that V0A amplitude is proportional to N_{part}
- conditional probability to measure amplitude n for a given N_{part}: $P(n|N_{part}) = P(n; N_{part}\mu, N_{part}k)$

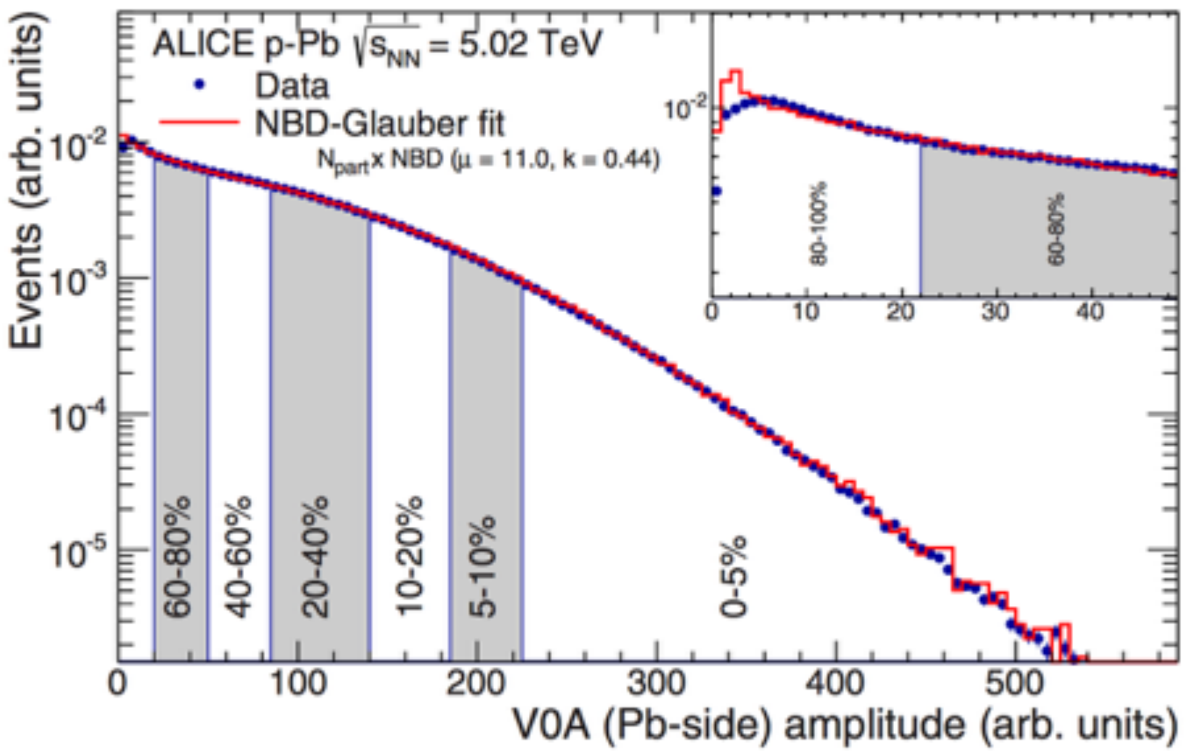

$$P(n; \mu, k) = \frac{\Gamma(n+k)}{\Gamma(n+1)\Gamma(k)} \cdot \frac{(\mu/k)^n}{(\mu/k+1)^{n+k}}$$

- convolution of Glauber N_{part} with $P(n|N_{part})$ to obtain calculated V0A distribution
- fit to the measured V0A distribution to obtain NBD parameters μ, k

Estimator	pp		p-Pb	
	μ	k	μ	k
V0A	9.6	0.56	11.0	0.44
CL1	9.8	0.64	8.74	0.76

Values of parameters μ, and k are similar to those obtained by fitting pp @ 7 TeV

Glauber-Gribov

Glauber-Gribov includes color fluctuations

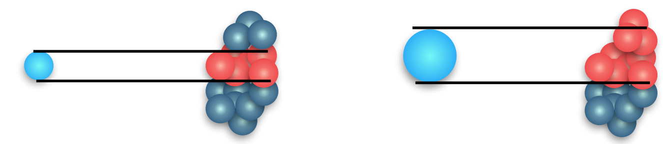

- event-by-event fluctuations in size of proton
- width of the fluctuation governed by parameter Ω (Ω=0 ◗ “standard” Glauber)
- changes π(N_{coll})

ALICE Coll., Phys. Rev. C 91 (2015) 064905

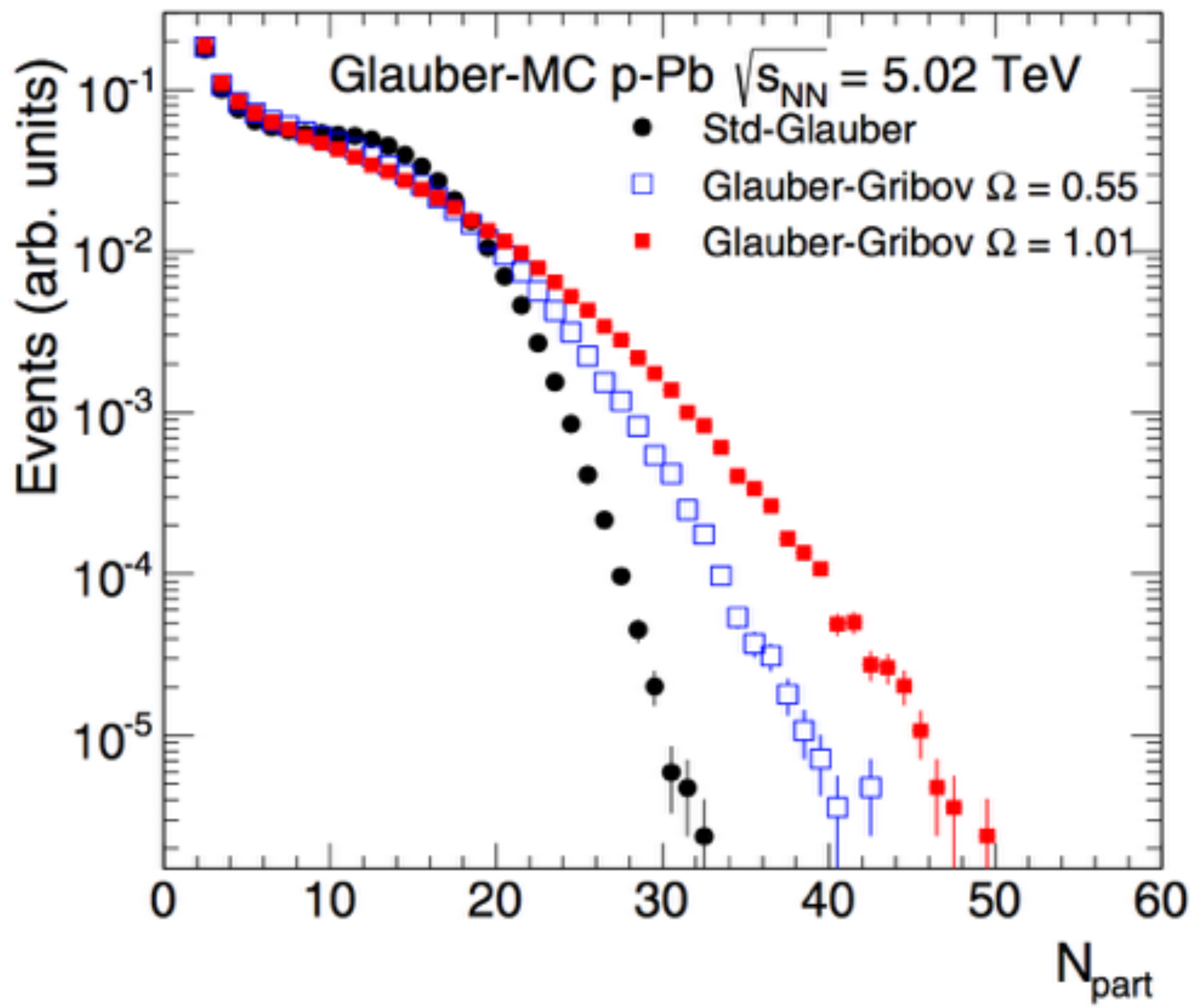

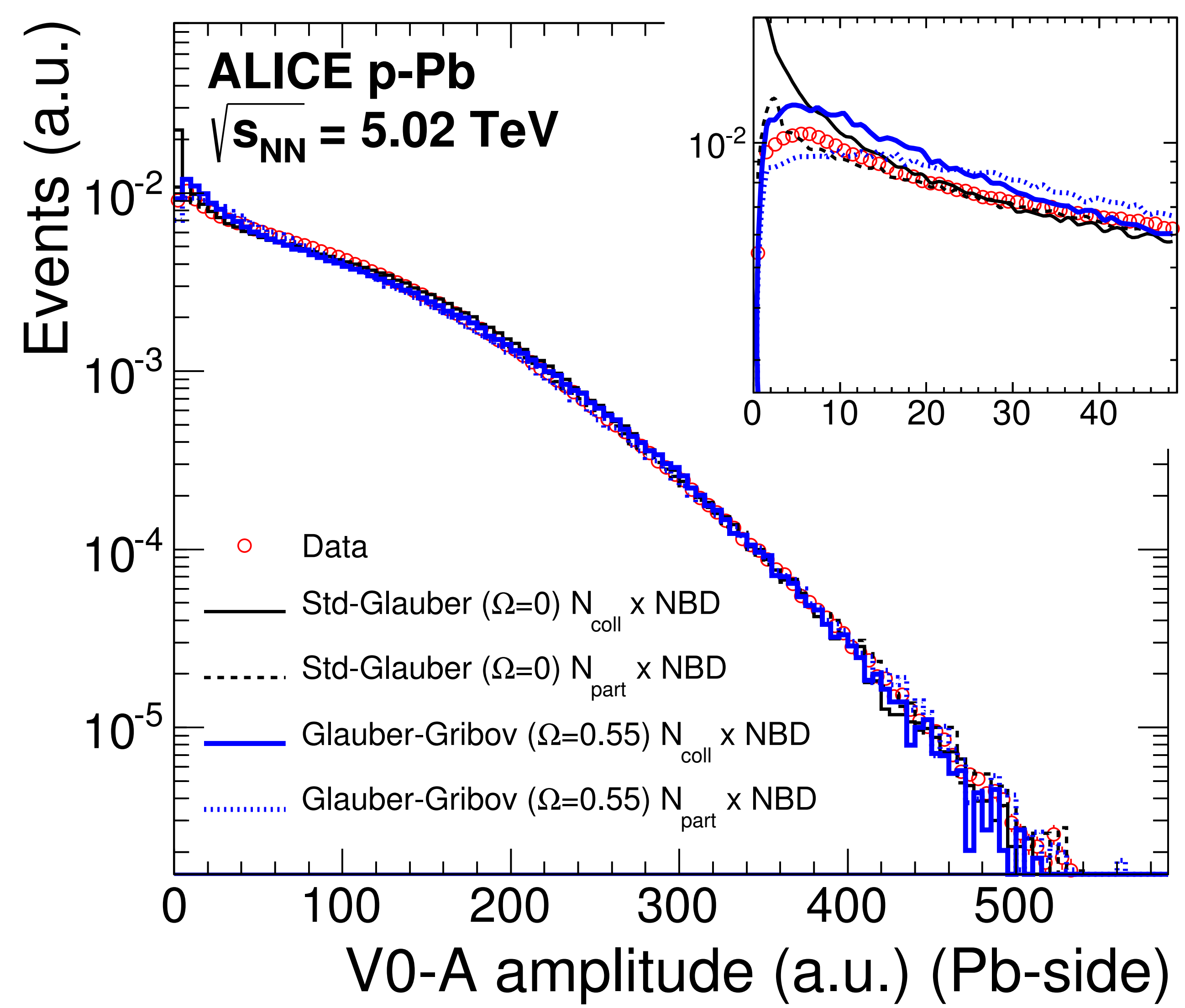

Consistency checks

Measurement of N_{coll} in separated y regions (ZNA and V0A inner ring) to establish their relation to centrality

➧ for centrality classes selected with ZN:

- P(N_{coll}) distributions in ZNA bins ⊗ NBD from Glauber fit to MB V0A multiplicity ➧ P(N_{coll})
- unfolding ➧ V0A distributions in ZNA centrality bins fit with P(N_{coll}) distribution ⊗ NBD from Glauber fit ➧ P(N_{coll})

  does not work for V0A distributions selected using a biased centrality estimator (CL1)

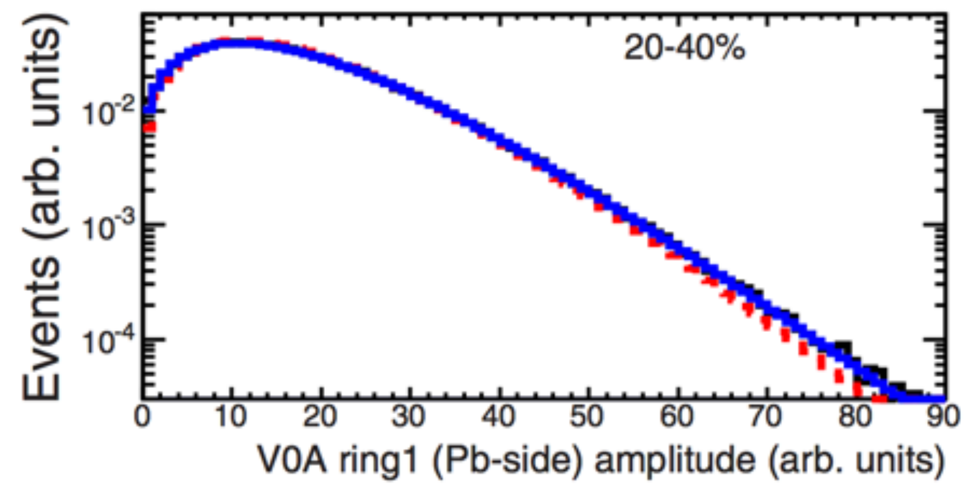

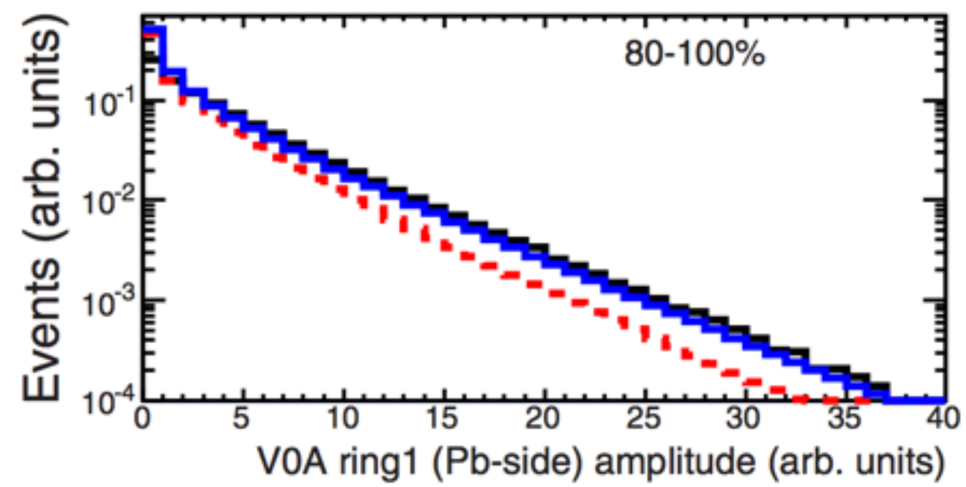

ALICE Coll., Phys. Rev. C 91 (2015) 064905

➧ energy measured by ZN is connected to the collision geometry

➧ ZN centrality selection does not induce a bias

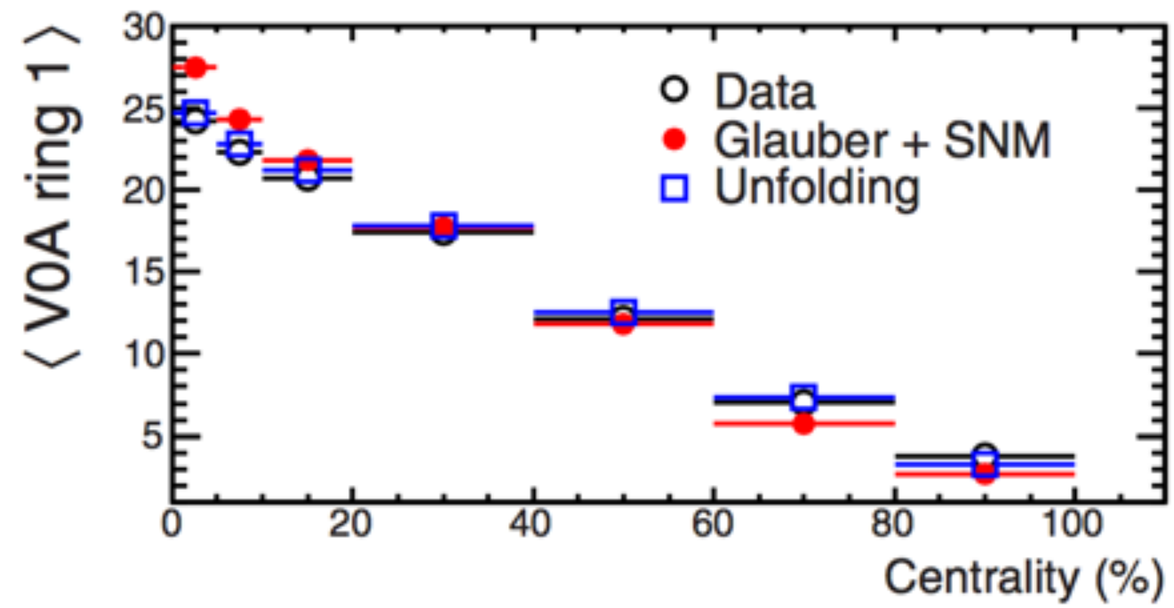

Slow nucleons

Hadron-nucleus collisions ➧ "slow" nucleon emission

"Black" and "gray" component
(terminology coming from emulsions experiments)

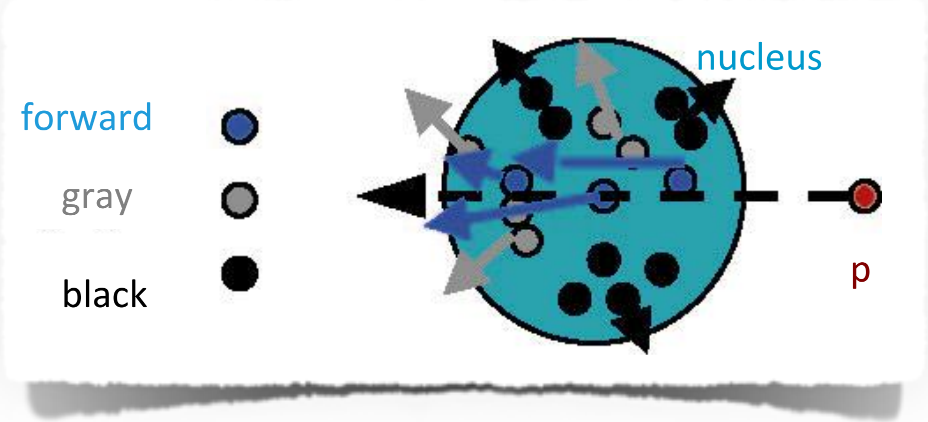

	β	p (MeV/c^2)
Black	0 ÷ 0.25	0 ÷ 250
Gray	0.25 ÷ 0.7	250 ÷ 1000

Black ➧ nucleons + low-energy target fragments from nuclear evaporation processes
Gray ➧ nucleons and light fragments emitted in the intra-nuclear cascade processes

F. Sikler, hep-ph/0304065

Features of slow nuclear emission weakly depend on hadron beam energy in a wide range (1 GeV - 1 TeV)

➧ slow particle emission mainly dictated by nuclear geometry

- kinematical distributions described by independent statistical emission from a moving frame
- isotropic emission from a source moving with velocity β
- number distribution of black/gray nucleons follows binomial distributions

SNM

No predictions for slow nucleon emission in p-A at LHC energies esist!

Model based on lower energy data

E910 Coll., Phys. Rev. C 60 024902 (1999)

Average no. of grey protons ➧ $\langle N_{grey,\,p}\rangle = c_0 + c_1 {*} N_{coll} + c_2 {*} N_{coll}$
the linear term is the dominant contribution (c_2~0)

A. Letourneau, Nucl. Phys. A 712 133 (2002)

Average no. of black protons ➧ $\langle N_{black,\,p}\rangle = 0.65 {*} \langle N_{grey,\,p}\rangle$

Average number of slow neutrons ➧

$$\langle N_{slown}\rangle = \alpha N_{LCF} + \left(a - \frac{b}{c + N_{LCF}}\right)$$

with:

N_{LCF} = no. of Light Charge fragments (Z<8) = $\gamma {*} \langle N_{slow,\,p}\rangle$ (γ = 1.75) ➧ ~ linear in N_{coll}
a = 50, b = 230, c = 4.2 (from a minimization procedure on LHC data) ➧ saturation term
α = 0.48 ➧ term linearly increasing in N_{coll}

ZN and ZP

ALICE Coll., Phys. Rev. C 91 (2015) 064905

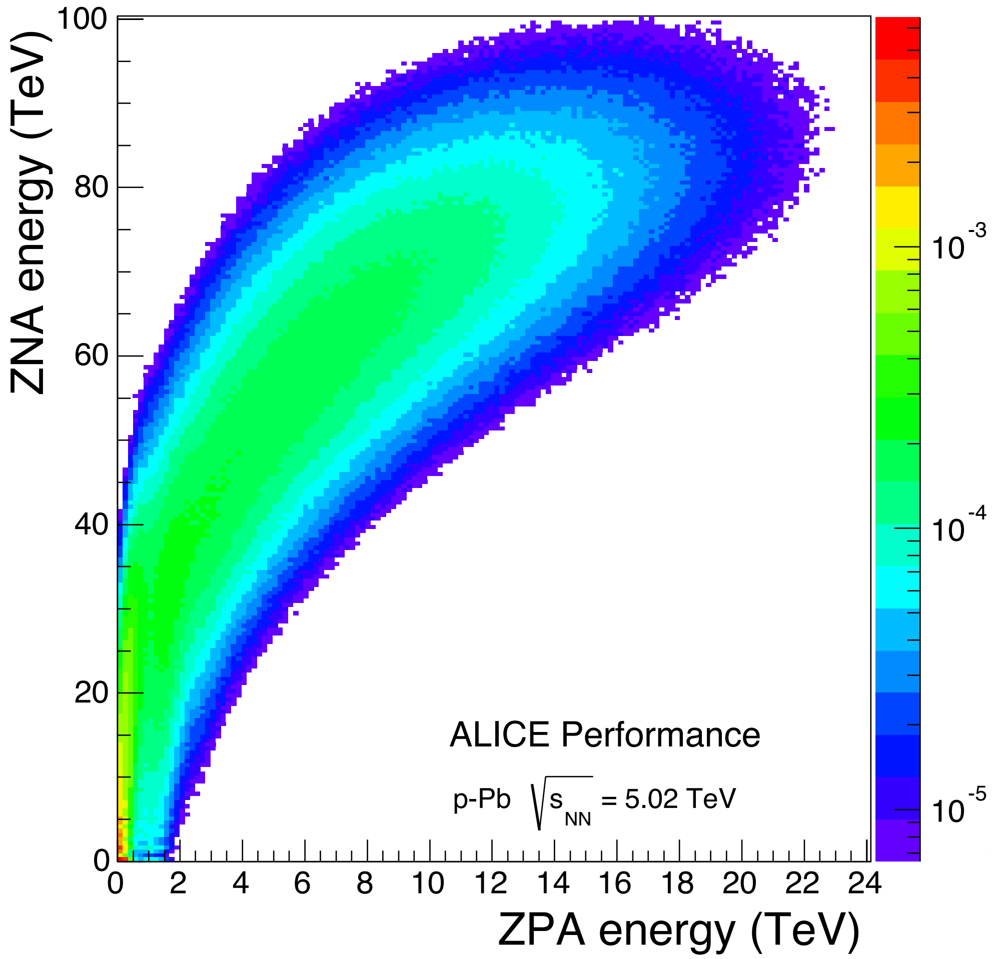

ZN vs. ZP energy on Pb-remnant side

- correlation up to the onset of a saturation in slow (black) neutron emission (same dependence as for lower energy data and for DPMJET+FLUKA MC at 5.02 TeV)
- ZN acceptance: 95.7%
- ZP acceptance: 82%
strongly affected by LHC optics parameters
detector response depends on proton impact point

DPMJET+FLUKA
p-Pb @ 5.02 TeV

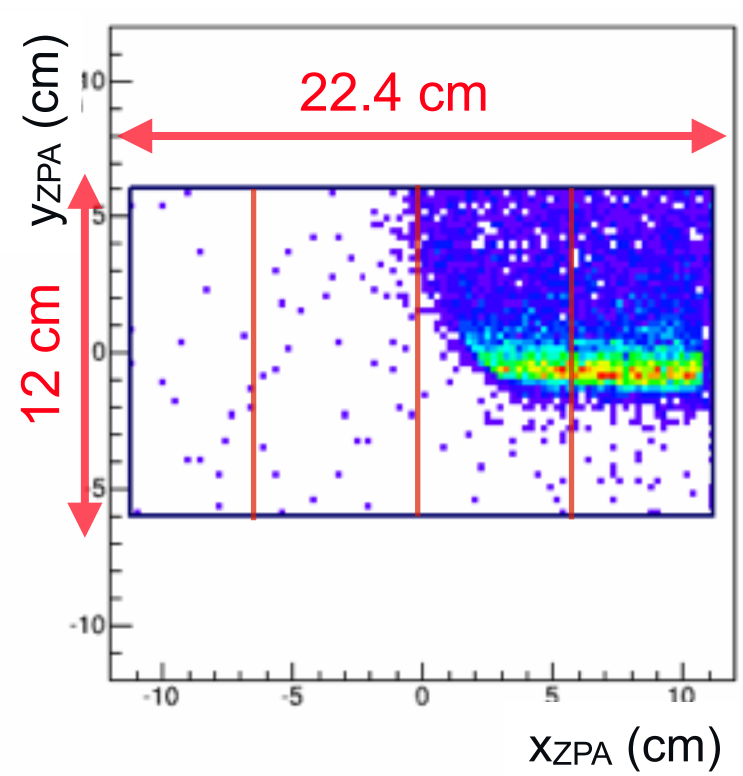

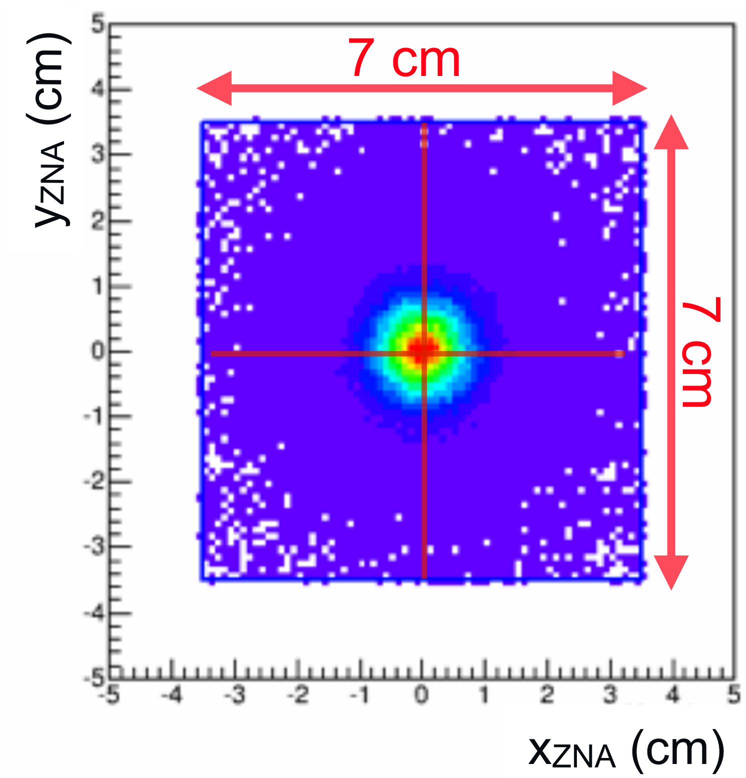

ZN: p and Pb-remnant side

ALICE Coll., Phys. Rev. C 91 (2015) 064905

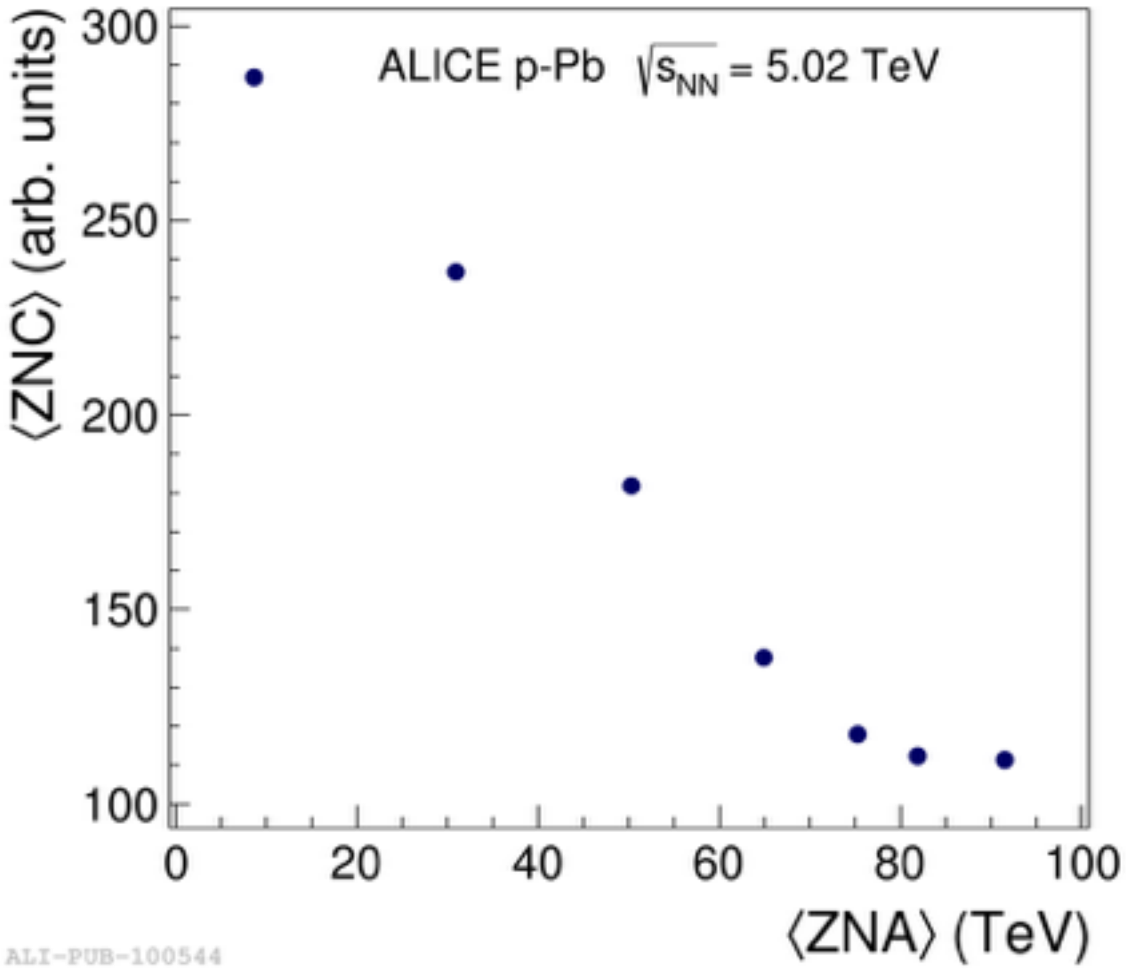

E_{ZNC} (p-side) is anti-correlated with E_{ZNA} (Pb-side)
➧ participant contribution can't be neglected for very peripheral collisions (while SNM assumes that for N_{coll}=0 no neutron is emitted!)

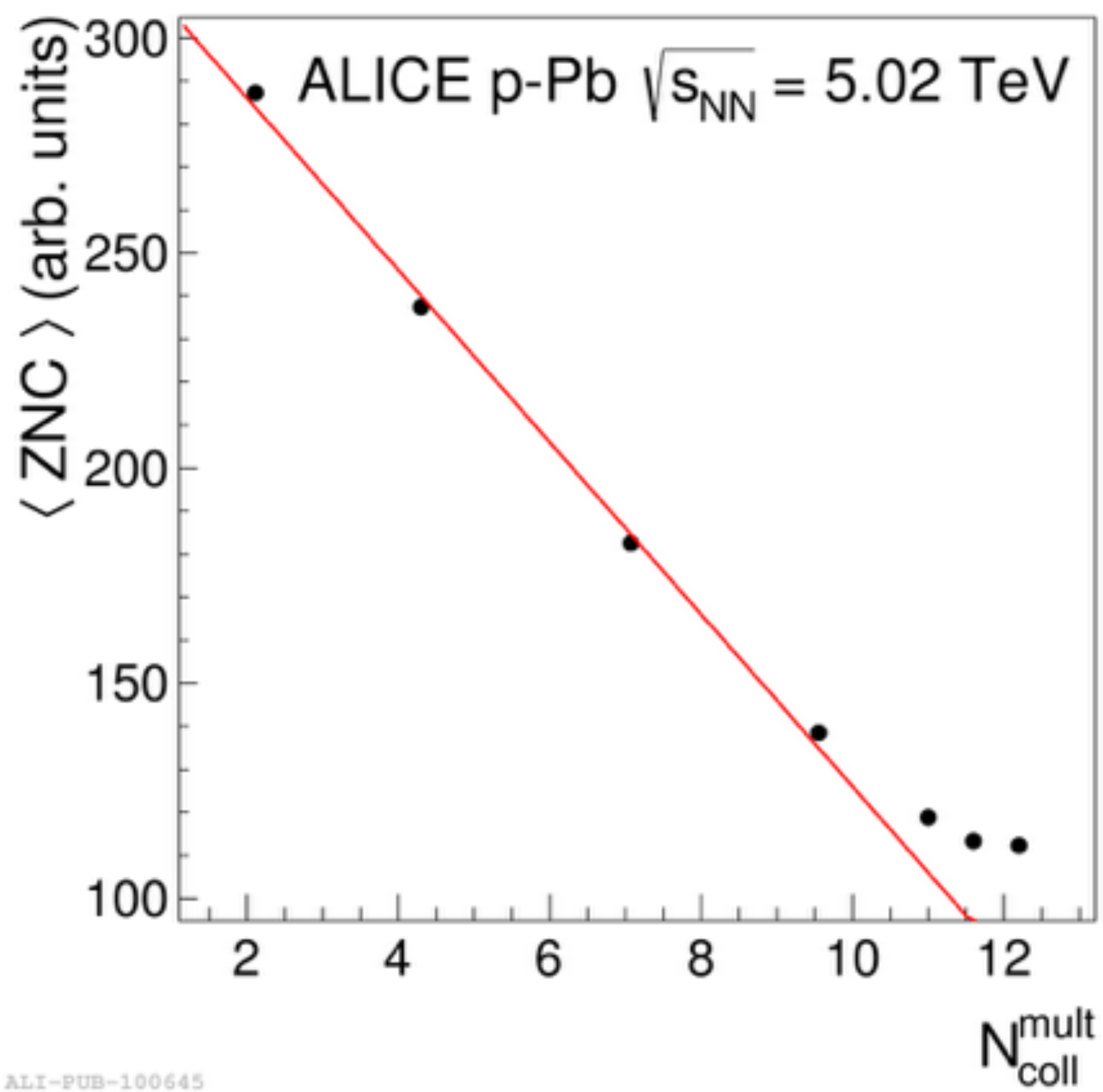

E_{ZNC} (p-side) vs. unbiased <N_{coll}>
➧ linear anti-correlation over a wide centrality range, consistently with a energy transfer from the proton proportional to N_{coll}

Normalized signals vs. multiplicity

ALICE Coll., Phys. Rev. C 91 (2015) 064905

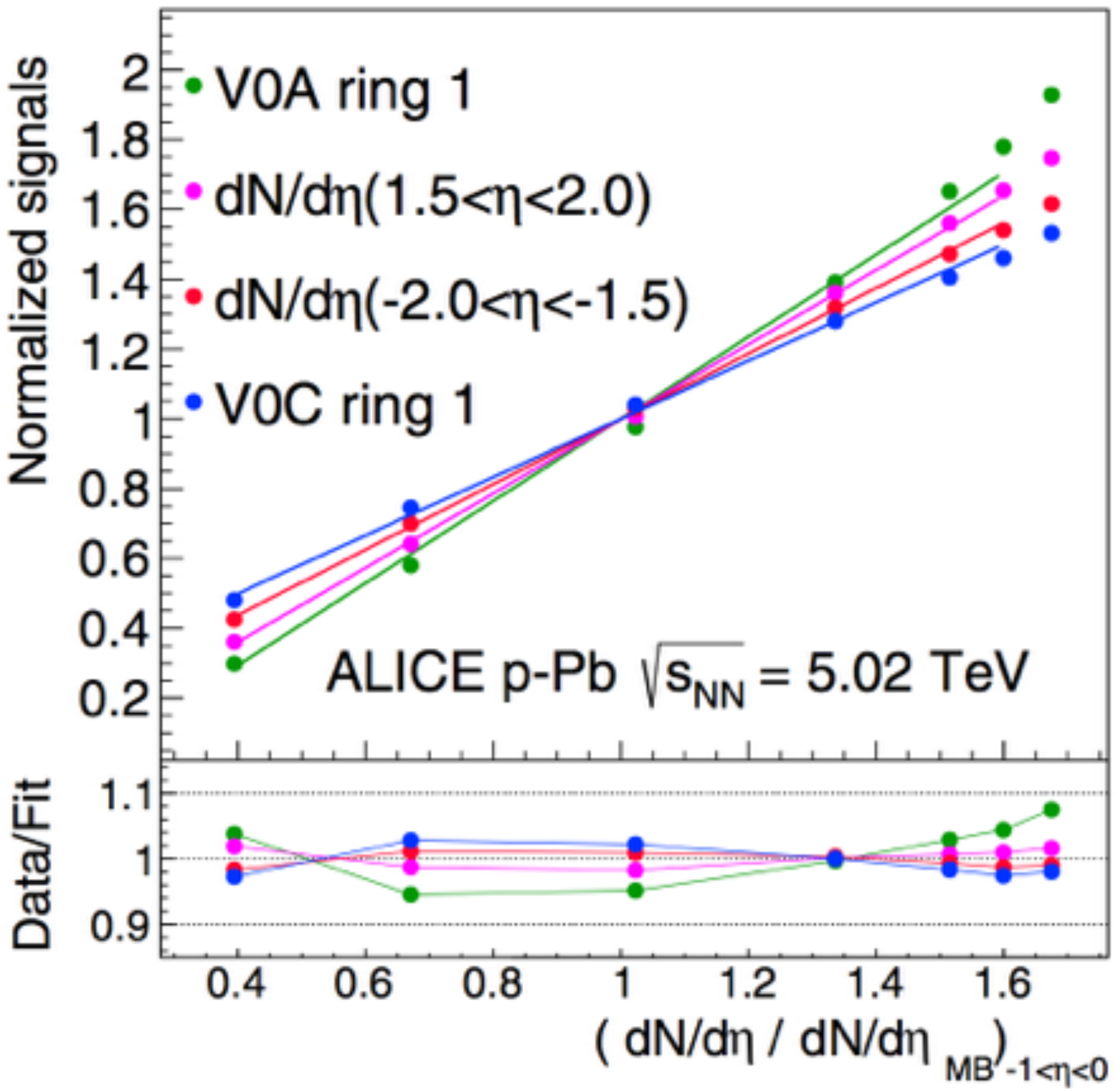

Self-normalized signals $\langle S\rangle_i/\langle S\rangle_{MB}$ in centrality bins selected by ZN vs. normalized charged particle density @ midrapidity

➧ clear η dependence of the slope

Wounded Nucleon Model (WNM)

➧ charged particle density @ midrapidity ~N_{part}
➧ at higher η predicts a dependence on a linear combination on N_{part}^{TARGET} and $N_{part}^{PROJECTILE}$ with coefficients which depend on η

➧ Observables related to N_{part} assuming a linear dependence parametrized with (N_{part}-α)
➧ Fit data with α free parameter ➧ α=0 means a perfect N_{part} scaling

$$\frac{<S>_i}{<S>_{MB}} = \frac{<N_{part}>_{MB}}{(<N_{part}>_{MB} - \alpha)} \cdot \left(\frac{<dN/d\eta>_i}{<dN/d\eta>_{MB}}\right)_{-1<\eta<0} - \frac{\alpha}{(<N_{part}>_{MB} - \alpha)}$$

Scaling vs. η

ALICE Coll., Phys. Rev. C 91 (2015) 064905

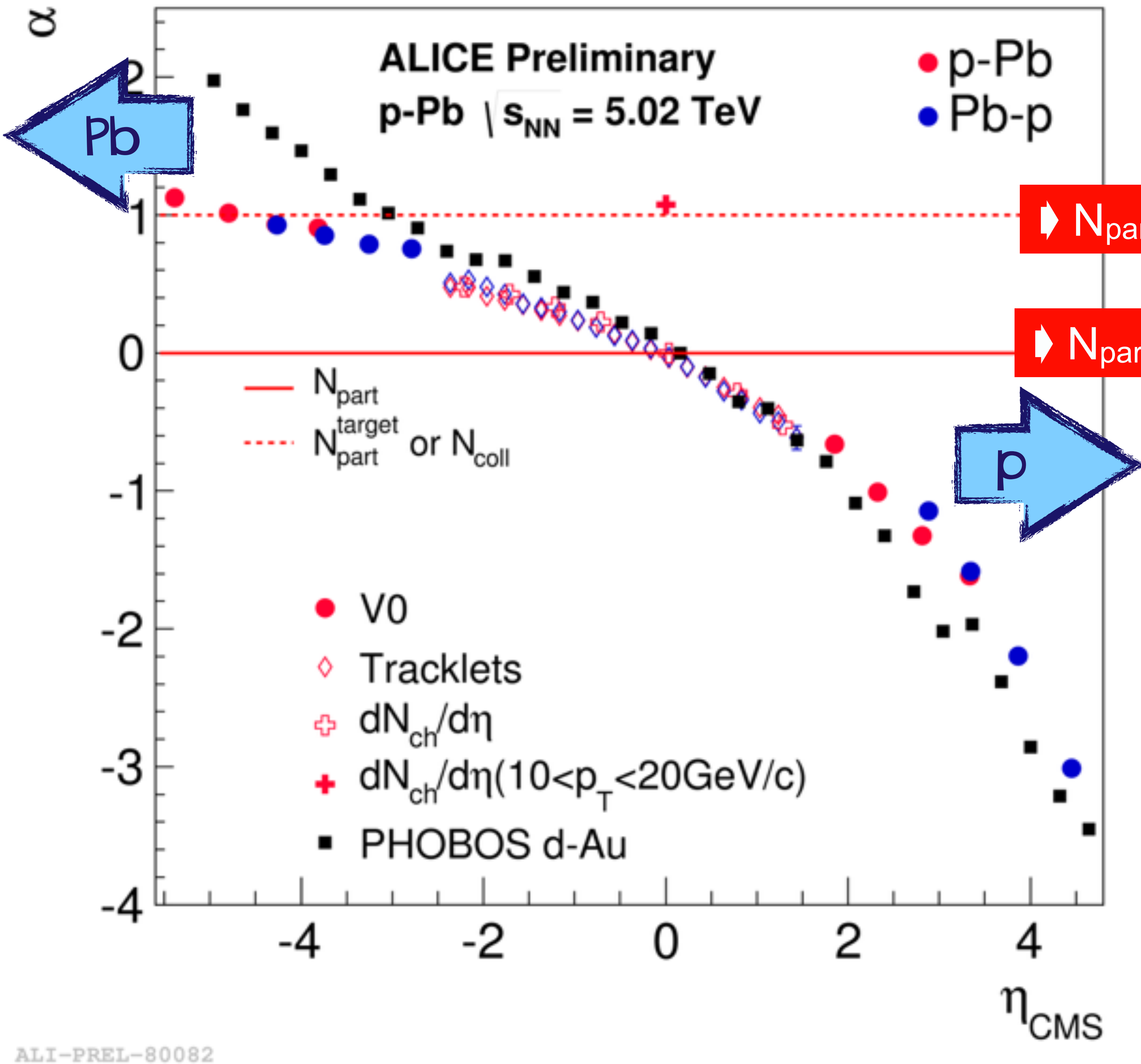

➧ $N_{part}-1 = N_{coll} = N_{part}^{Pb}$ scaling

➧ N_{part} scaling

α parameter values vs. η_{CMS}

α=0 ➧ N_{part} scaling

➧ clear η dependence of particle production

➧ in the Pb-going direction, α reaches the value obtained for high p_T particle production:

α=1 ➧ $N_{part}^{Pb} = N_{part}-1 = N_{coll}$ scaling

N_{ch}/N_{part}

ALICE Coll., Phys. Rev. C 91 (2015) 064905

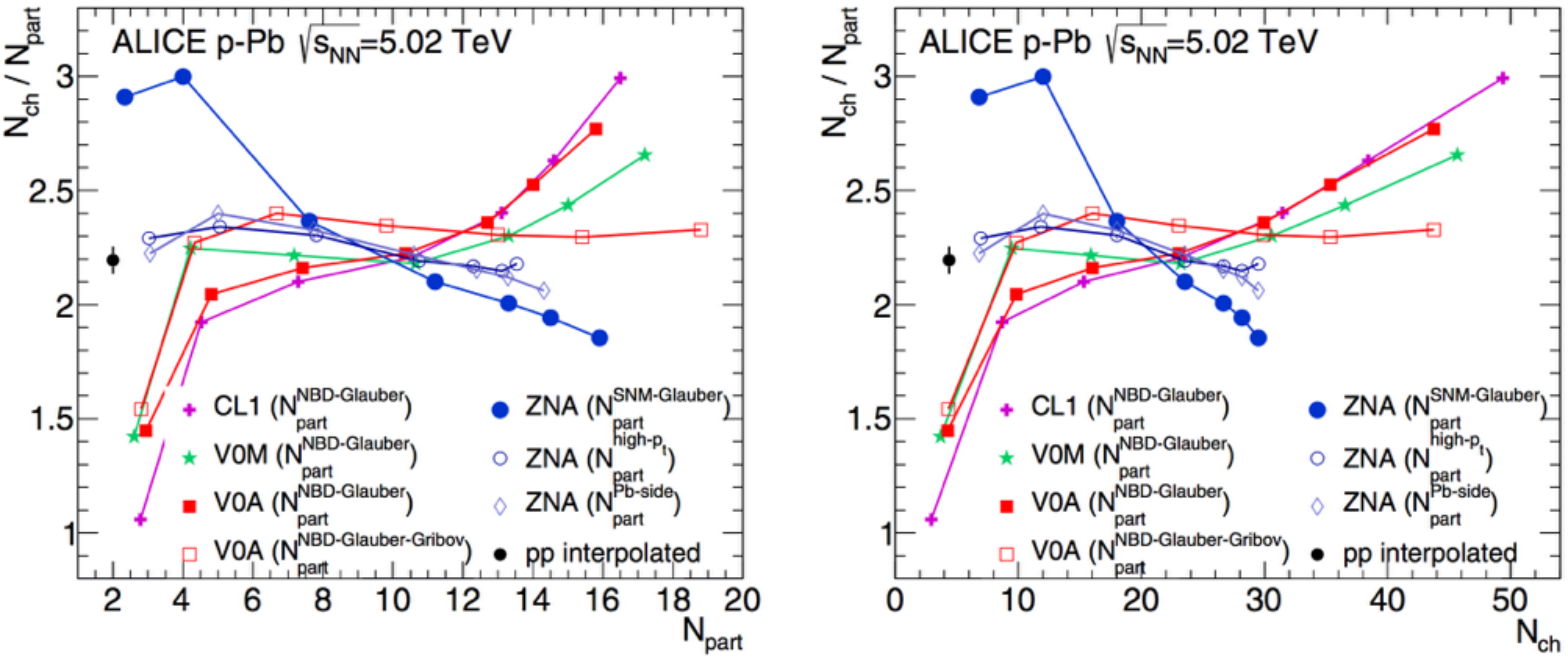

Long-range correlations

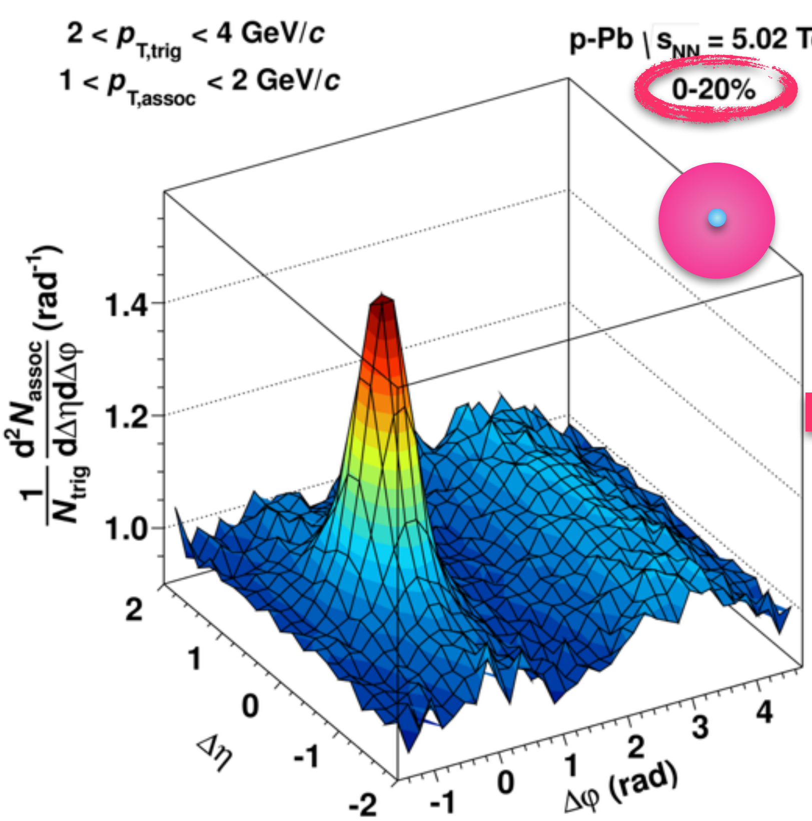

−

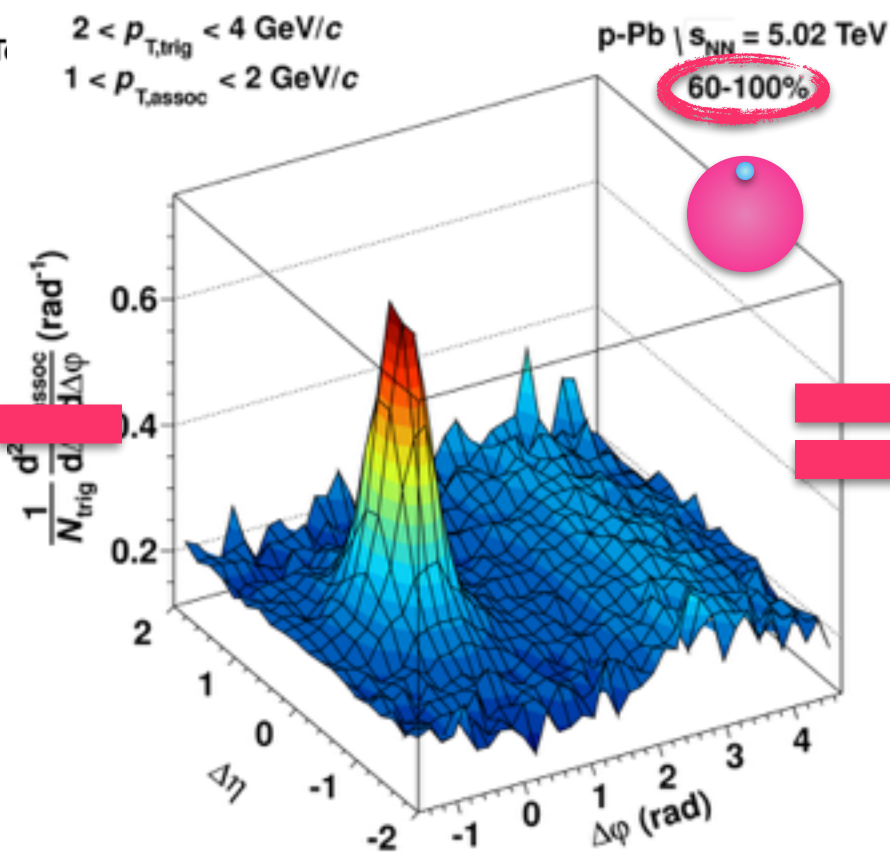

=

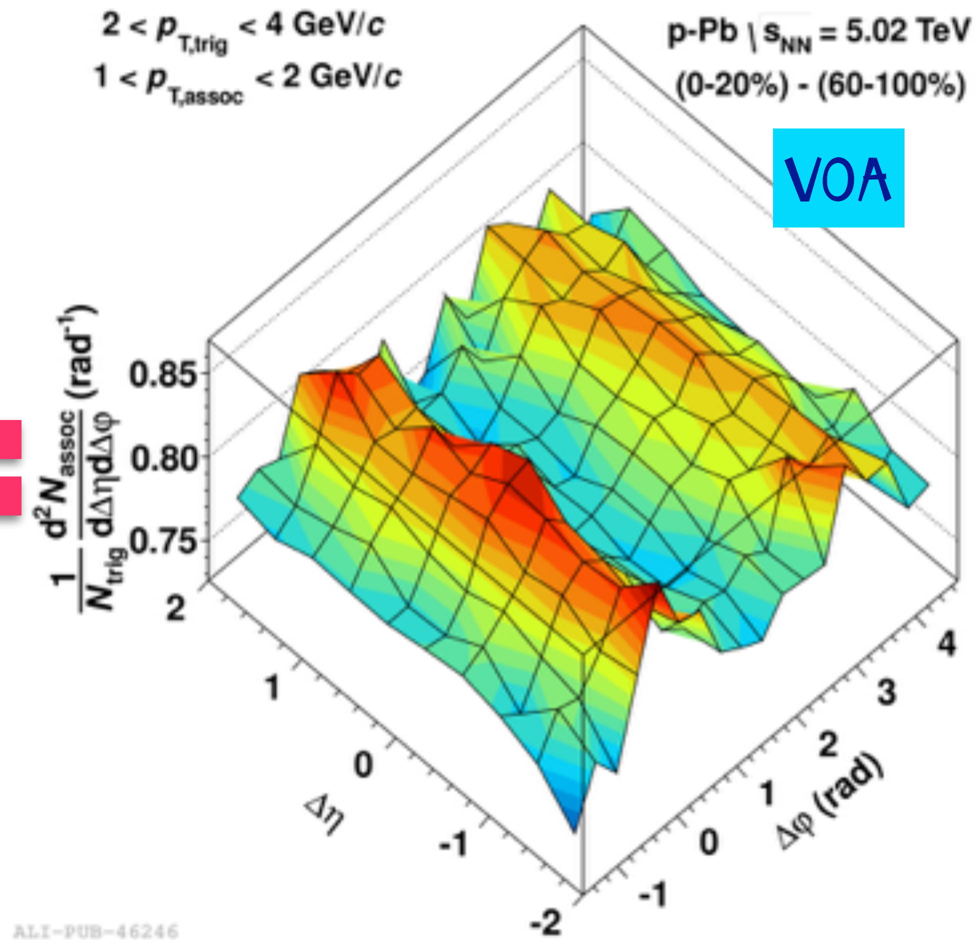

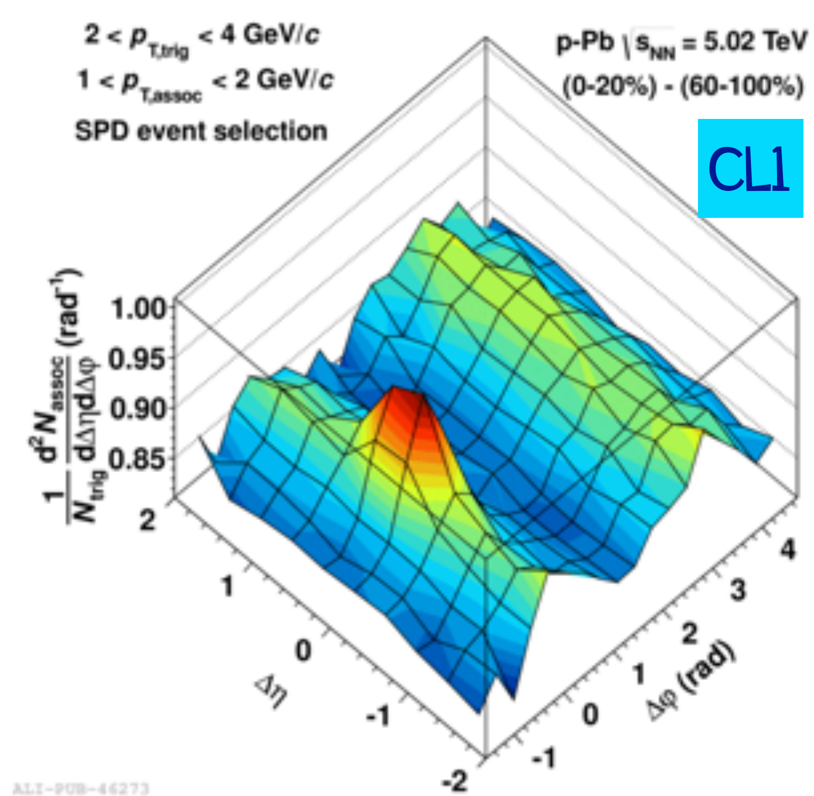

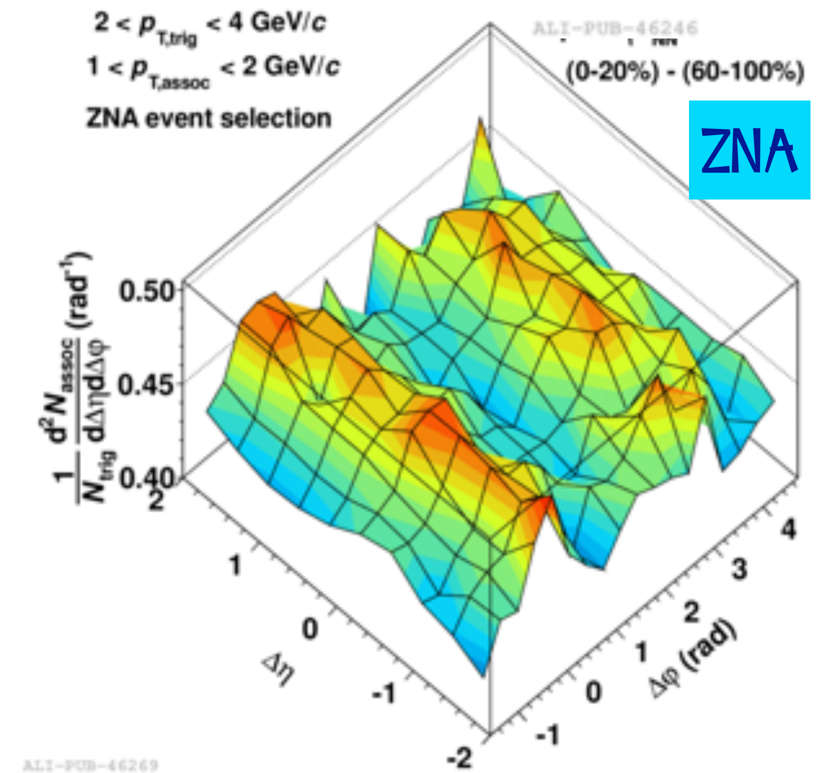

ALICE Coll., PLB 719 (2013) 29

Long range correlation subtraction

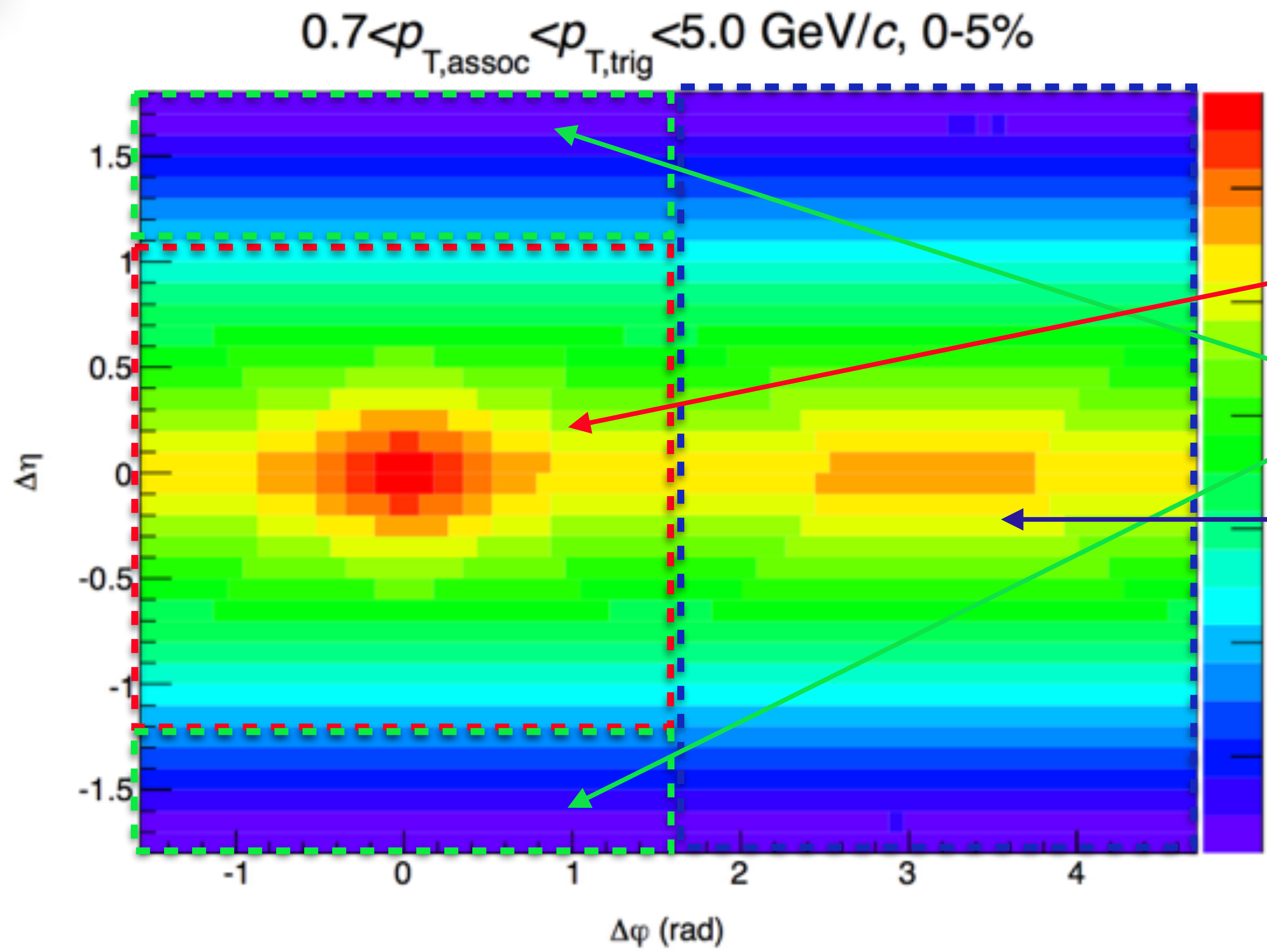

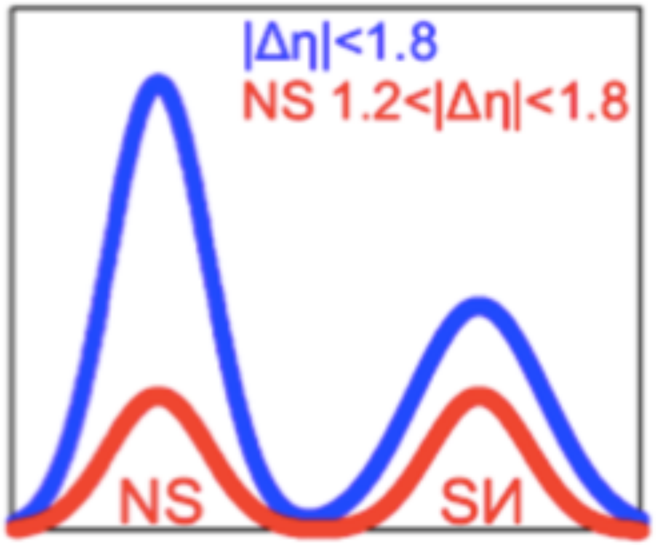

NS ➧ divided in short-range $|\Delta\eta|<1.2$ and long-range $1.2<|\Delta\eta|<1.8$ regions ➧ normalized and subtracted from one another

AS ➧ jet and ridge contributions can't be disentangled ➧ NS long-range correlation mirrored around $\Delta\varphi=\pi/2$ and subtracted from AS

NS and AS yield per trigger particle